Prepared for submission to JHEP

# Baryogenesis

**Marieke Postma**

*Nikhef, Theory Group, Science Park 105, 1098 XG, Amsterdam, The Netherlands*
*Radboud University Nijmegen, IMAPP, Heyendaalseweg 135, Nijmegen, the Netherlands*

*E-mail:* mpostma@nikhef.nl

Abstract: These notes on baryogenesis discuss the Sakharov conditions, and the basics of leptogenesis and electroweak baryogenesis.

## Contents

# 1 Introduction

The Standard Model (SM) interactions are the same for particles and antiparticles, except for the small CP violating phase in the CKM matrix (and possibly a tiny $\theta$-angle). Yet, everything we see around us is made of matter. Cosmic rays are consistent with matter primaries. There seem to be no anti-matter regions in the universe, as we would have seen gamma-rays from the boundaries from annihilating matter and antimatter.

The asymmetry between matter and antimatter, or between baryons and anti-baryons, is characterized by the ratio of densities of baryon number and entropy ($s = \frac{2\pi}{45} g_{*s} T^3$); this ratio has been determined by two independent methods

$$Y_b = \frac{n_b - n_{\bar{b}}}{s} = \frac{1}{7.04} \frac{n_b - n_{\bar{b}}}{n_\gamma} = \begin{cases} 8.2 - 9.4 \times 10^{-11} & \text{BBN} \\ 8.65 \pm 0.09 \times 10^{-11} & \text{CMB} \end{cases} \tag{1.1}$$

with $n_{\bar{b}} \approx 0$. For every $10^{10}$ photons in the universe there is one baryon. During adiabatic expansion of the universe $\mathrm{d}S = 0$ and the ratio $Y_b$ remains constant.

Big bang nucleosynthesis (BBN) is the period where the light elements, such as deuterium, helium and lithium, are formed. The priomordial abundances of these elements, which can be observed in todays universe, depend sensitively on the ratio of baryons to photons at BBN. Energetic photons can dissociate light elements, and the larger $\eta$ the earlier BBN starts. The amount of baryons can be extracted from cosmic microwave background measurements as follows. Over densities grow under the action of gravity, and eventually collapse. The collapse is reverted by the photon pressure of the plasma, and this leads to the accoustic oscillations observed in the CMB spectrum. The baryons provide the mass for the collapsing and expanding matter, whereas the photons provide the pressure, and the amount of baryons thus influence the height of the accoustic peaks.

The asymmetry cannot be an initial condition of the universe if inflation took place. Inflation erases all initial information. During inflation the universe grows by an enormous amount (larger than $a_f/a_i = e^{3N}$ with $N \gtrsim 50$) and all number densities drop to zero as they are suppressed by the volume factor. So at then end of inflation the universe is basically empty and filled with false vacuum energy. Somewhere between the end of inflation and today the baryon asymmetry must have been created.

There are many baryogenesis scenarios that provide a dynamical origin for the baryon assymetry on the market: GUT baryogenesis, baryogenesis from primordial black holes, Affleck-Dine (AD) baryogenesis, baryogenesis at preheating, baryogenesis via leptogenesis, spontaneous baryogenesis, gravitational baryogenesis, defect mediated baryogenesis, B-ball baryogenesis, baryogenesis from CPT breaking, baryogenesis

through quantum gravity, axiogenesis, baryogenesis by brane collision, mesogenesis, electroweak baryogenesis, etc. And many of these are collective names for whole classes of models and implementations.

Arguably the best motivated scenario is leptogenesis, as it only requires the addition of right-handed neutrinos on top of the SM, which are anyway needed to give the neutrinos a mass. Unfortunately, in the standard vanilla implementation the right-handed neutrinos are heavy and out of reach of experiments. One of the few scenarios that can be tested and falsified is electroweak (EW) baryogenesis, which requires new physics at the EW scale, and thus can be probed by colliders, precision EDM experiments and, in the future, gravitational wave observations.

Plan of the lectures:

- Sakharov conditions
- Leptogenesis
- Electroweak baryogenesis

### 1.1 References

All references are missing from this notes. I'll list here some references to review papers, in which all references to the original literature can be found. Review papers on baryogenesis are [1, 2, 2, 3], on leptogenesis [4–6], on thermal field theory [7, 8], on tunneling [9] and on electroweak baryogenesis [10–12].

## 2 Sakharov conditions

Sakharov was the first to describe a dynamical baryogenesis mechanism, and his paper from 1967[1] contains three neccesary conditions for any baryogenesis scenario.

1. Baryon number violation. If all reactions/processes have as many baryons in the initial as in the final state, no asymmetry will be created.

2. C and CP violation. C violation is needed, else the rate for particle creation is the same as that for antiparticle creation. CP violation is needed, else the rate for left-chiral particle creation is the same as that for right-chiral antiparticles.

[1] In those days baryon number was thought to be a good quantum number and the asymmetry was explained as an initial condition of the universe. This changed with the realization of the chiral anomaly, GUT theories, and black hole evaporation – which all lead to baryon number violation – and the theory of inflation. Sakharov's paper was not cited until 1979.

3. Departure from thermal equilibrium. If all the particles in the universe remain in thermal equilibrium, then no preferred direction for time can be defined.

Baryon number is odd under C and CP. A non-zero expectation value $\langle B\rangle$ requires that the Hamiltonian $H$ violates both C and CP. Let's see this explicitly in the SM. The SM is classically invariant under the global $U(1)$ transformation $q(x) \to e^{i\epsilon/3}q(x)$ and $\bar{q}(x) \to e^{-i\epsilon/3}\bar{q}(x)$ for the quarks and antiquarks (and all other fields do not transform). Noether's theorem gives the associated baryon current and charge

$$\partial^\mu J^B_\mu = \partial^\mu \sum_q \frac{1}{3}\bar{q}\gamma_\mu q = 0 \quad \Rightarrow \quad B = \int \mathrm{d}^3x\, J^B_0(x) = \sum_q \frac{1}{3}\int \mathrm{d}^3x\, \bar{q}\gamma_0 q, \tag{2.1}$$

The quark fields transfrom under P and C as

$$\begin{aligned} Pq(\mathbf{x},t)P^{-1} &= \gamma^0 q(-\mathbf{x},t), \\ Cq(\mathbf{x},t)C^{-1} &= -i\gamma^2 q^*(\mathbf{x},t), \end{aligned} \tag{2.2}$$

with $\gamma^0$, $\gamma^2$, and $\gamma_5 = i\gamma^0\gamma^1\gamma^2\gamma^3$ the Dirac matrices. The expressions on the rhs $\gamma^0 q(-\mathbf{x},t)$ and $i\gamma^2 q^*(\mathbf{x},t)$ satisfy the Dirac equation with respectively momentum and charge flipped; the overall sign is a phase convention. Then $q^\dagger q$ transforms as

$$Pq^\dagger(\mathbf{x},t)q(\mathbf{x},t)P^{-1} = q^\dagger(-\mathbf{x},t)q(-\mathbf{x},t), \tag{2.3}$$

$$\begin{aligned} Cq^\dagger(\mathbf{x},t)q(\mathbf{x},t)C^{-1} &= (-i\gamma^2 q(\mathbf{x},t))^T(-i\gamma^2 q^*(\mathbf{x},t)) = q^T(\mathbf{x},t)q^*(\mathbf{x},t) \\ &= -(q^\dagger(\mathbf{x},t)q(\mathbf{x},t))^T = -q^\dagger(\mathbf{x},t)q(\mathbf{x},t) \end{aligned} \tag{2.4}$$

where the sign on the last line enters from interchanging fermion fields. Since baryon number is obtained integrating $q^\dagger q$ over spatial coordinates, it follows that baryon number is even under P and odd under C

$$PBP^{-1} = B, \qquad CBC^{-1} = -B. \tag{2.5}$$

The need for deviation of thermal equilibrium can be proven as follows. Note first that the baryon expectation value in thermal equilibrium $\langle B(t)\rangle_T = \mathrm{tr}(\rho B(t))$ is constant in time; here $\rho = \mathrm{e}^{-H/T}$ is the density operator. Using the unitary time evolation operator we then have

$$\langle B(t)\rangle_T = \mathrm{tr}(\mathrm{e}^{-H/T}\mathrm{e}^{iHt}B(0)\mathrm{e}^{-iHt}) = \mathrm{tr}(\mathrm{e}^{-iHt}\mathrm{e}^{-H/T}\mathrm{e}^{iHt}B(0)) = \langle B(0)\rangle_T \tag{2.6}$$

Now $B(0)$ is even under $T$ (as $X(t) \xrightarrow{T} X(-t)$), and as we saw in eq. (2.5) odd under CP. It is thus odd under $\Theta = CPT$. In thermal equilibrium we then find that $B(t)$

must vanish

$$\langle B(t)\rangle_T = \mathrm{tr}(\mathrm{e}^{-H/T}B(0)) = \mathrm{tr}(\Theta^{-1}\Theta e^{-H/T}B(0)) = \mathrm{tr}(\mathrm{e}^{-H/T}\Theta B(0)\Theta^{-1}) = -\langle B(t)\rangle_T, \tag{2.7}$$

where we used that the Hamiltonian is CPT invariant.

It is subtle how baryon number vanishes in thermal equilibrium. Consider the baryon number violating decay $X \to qq$. If C and CP are violated the decays rates of $X$ and $\bar{X}$ differ

$$\Gamma(X \to qq) = \Gamma_0(1+\epsilon), \qquad \Gamma(\bar{X} \to \bar{q}\bar{q}) = \Gamma_0(1-\epsilon) \tag{2.8}$$

The decays generate a non-zero baryon number. One might think that using detailed balance, that the inverse decay $qq \to X$ is more likely than $\bar{q}\bar{q} \to \bar{X}$, thus erasing baryon number. However, detailed balance is based on T invariance, which is broken in the presence of CP violation (by CPT invariance), and cannot be used. In fact, CPT tells that the inverse decays are

$$\Gamma(qq \to X) = \Gamma_0(1-\epsilon), \qquad \Gamma(\bar{q}\bar{q} \to \bar{X}) = \Gamma_0(1+\epsilon), \tag{2.9}$$

exactly the opposite. How then is baryon number restored?

Well, B violation tells that there should be a competing decay channel $X \to Y$ with $Y$ having different baryon number than the quark pair; otherwise we could simply assign $X$ the same baryon number as the quark pair, and $B$ is not violated in the decay. CPT assures that the total decay rate of $X$ and $\bar{X}$ are the same

$$\Gamma(X \to qq) + \Gamma(X \to Y) = \Gamma(\bar{X} \to \bar{q}\bar{q}) + \Gamma(\bar{X} \to \bar{Y}) \tag{2.10}$$

The additional $Y \leftrightarrow qq$ interactions then wash out the asymmetry.

## 2.1 Sakharov conditions in the SM

### 2.1.1 Review of the SM

We begin by defining the SM Lagrangian. We write the Lagrangian in terms of left handed quark and lepton doublets, $q_L$, and, $l_L$, respectively, and right-handed singlets $u_R$, $d_R$, and $e_R$. The field $H$ represents the $SU_L(2)$ Higgs doublet of scalar fields $H^a$. We define $\tilde{H}^a = \epsilon^{ab}H^{b*}$, where $\epsilon^{ab}$ is the antisymmetric tensor in two dimensions ($\epsilon^{12} = +1$). The covariant derivative is given by

$$D_\mu = \partial_\mu - i\frac{g_s}{2}G^a_\mu\lambda^a - i\frac{g}{2}W^i_\mu\tau^i - ig'YB_\mu\,, \tag{2.11}$$

where $g_s$, $g$, and $g'$ are, respectively, the $SU_c(3)$, $SU_L(2)$, and $U_Y(1)$ coupling constants. $\lambda^a/2$ and $\tau^i/2$ denote $SU(3)$ and $SU(2)$ generators, in the representation of the field on

which the derivative acts. The hypercharge assignments, $Y$, are $1/6$, $2/3$, $-1/3$, $-1/2$, $-1$, and $1/2$ for $q_L$, $u_R$, $d_R$, $l_L$, $e_R$, and $H$, respectively. The field strengths are

$$\begin{aligned} G^a_{\mu\nu} &= \partial_\mu G^a_\nu - \partial_\nu G^a_\mu - g_s f^{abc} G^b_\mu G^c_\nu \,, \\ W^i_{\mu\nu} &= \partial_\mu W^i_\nu - \partial_\nu W^i_\mu - g\epsilon^{ijk} W^j_\mu W^k_\nu \,, \\ B_{\mu\nu} &= \partial_\mu B_\nu - \partial_\nu B_\mu \,, \end{aligned} \tag{2.12}$$

with $f^{abc}$ and $\epsilon^{ijk}$ denoting the $SU(3)$ and $SU(2)$ structure constants.

The SM Lagrangian is then written as

$$\begin{aligned} \mathcal{L}_{SM} = (D_\mu H)^\dagger D^\mu H - \lambda(H^\dagger H - \frac{1}{2}v^2)^2 - \Big(\bar{q}_L Y_u \tilde{H}\, u_R - \bar{q}_L Y_d H\, d_R + \bar{l}_L Y_e H\, e_R + \text{h.c.}\Big) \\ - \frac{1}{4}\left(G^a_{\mu\nu} G^{a\,\mu\nu} + W^i_{\mu\nu} W^{i\,\mu\nu} + B_{\mu\nu} B^{\mu\nu}\right) + \sum \bar{\psi} i \not{D}\, \psi. \end{aligned} \tag{2.13}$$

where the sum in the last term is over all fermions $\psi = \{q_L, u_R, d_R, l_L, e_R\}$. The terms on the first line are the Higgs kinetic term, the Higgs potential, and the yukawa interactions, whereas the 2nd line gives the kinetic terms for the gauge fields and the fermions. We parameterize the Higgs doublet

$$H = \frac{1}{\sqrt{2}} \begin{pmatrix} \theta_2 + i\theta_3 \\ \phi + h + i\theta_1 \end{pmatrix} \tag{2.14}$$

with $\phi$ the classical background, and $h$ and $\theta_i$ the Higgs and Goldstone boson fluctuations. Expanding around the background $\mathcal{L}^{(0)}$ gives the classical potential

$$V_0 = -\mathcal{L}^{(0)} = \frac{\lambda}{4}(\phi^2 - v^2)^2 \tag{2.15}$$

with $\mu^2 = \lambda v^2$. The potential is minimized at $\phi_0 = v = 246\,\text{GeV}$. The vacuum Higgs mass $\partial^2 V|_{\phi=v} = m_\phi^2 = 2\lambda v^2 = (125\,\text{GeV})^2$, from which it follows $\lambda = \frac{1}{2}(m_H/v)^2 \approx 0.12$.

The classical Higgs background breaks the EW symmetry and gives masses to the EW bosons. This can be seen by working out the covariant derivatives of the Higgs field kinetic term

$$\begin{aligned} \mathcal{L} \supset (D_\mu H)(D^\mu H)^\dagger &= \frac{1}{2}\begin{pmatrix} 0 & \phi \end{pmatrix} (g W^a_\mu \tau^a + \frac{1}{2} g' B_\mu)(g W^{b\mu} \tau^b + \frac{1}{2} g' B^\mu) \begin{pmatrix} 0 \\ \phi \end{pmatrix} + ... \\ &= \frac{1}{2}\frac{\phi^2}{4}\left[g^2 (W^1)^2 + g^2 (W^2)^2 + (-g W^3 + g' B)^2\right] \\ &= \frac{\phi^2}{4}\left[(g^2 + g'^2)\frac{1}{2} Z^2 + g^2 W^+ W^-\right] \end{aligned} \tag{2.16}$$

We defined the mass eigenstates

$$Z = \frac{1}{\sqrt{g'^2+g^2}}(gW_3 - g'B), \quad A_\gamma = \frac{1}{\sqrt{g'^2+g^2}}(gW_3 + g'B), \quad W^\pm = \frac{1}{\sqrt{2}}(W^1 \mp W^2) \tag{2.17}$$

with masses

$$\{m_Z, m_W, m_\gamma\} = \{\sqrt{g'^2+g^2}\frac{\phi}{2}, g\frac{\phi}{2}, 0\} \tag{2.18}$$

We can rewrite the gauge interactions in the fermion kinetic terms in terms of the gauge boson mass eigenstates

$$\mathcal{L}_{SM} \supset \sum \bar{\psi} i \not{D} \psi = g(W^+_\mu J^{\mu+}_W + W^-_\mu J^{\mu-}_W + Z_\mu J^\mu_z) + eA^\mu_\gamma J^\mu_{\rm EM} + ... \tag{2.19}$$

with $e = gg'/\sqrt{g^2+g'^2}$ the electric charge. The currents are

$$\begin{aligned} J^{\mu+}_W &= \frac{1}{\sqrt{2}}(\bar{\nu}_L \gamma^\mu e_L + \bar{u}_L \gamma^\mu d_L), & J^{\mu-}_W &= \frac{1}{\sqrt{2}}(\bar{e}_L \gamma^\mu \nu_L + \bar{d}_L \gamma^\mu u_L) \\ J^\mu_Z &= \cos^{-1}\theta_W \sum_f q^Z_f \bar{f}\gamma^\mu f, & J^\mu_{\rm EM} &= \sum_f q^{\rm EM}_f \bar{f}\gamma^\mu f, \end{aligned} \tag{2.20}$$

with $\cos\theta_W = g/\sqrt{g^2+g'^2}$ and $q^Z, q^{\rm EM}$ the $Z$ and electric charges of the fermions.

Fermion masses arise from the yukawa interactions. In the Higgs background

$$\begin{aligned} \mathcal{L} &\supset -\left(\bar{q}_L Y_u \tilde{H}\, u_R + \bar{q}_L Y_d H\, d_R + \bar{l}_L Y_e H\, e_R + \text{h.c.}\right) \\ &= -\left(\frac{1}{\sqrt{2}} Y_u \phi \bar{u}_L u_R + \frac{1}{\sqrt{2}} Y_d \phi \bar{d}_L d_R + \frac{1}{\sqrt{2}} Y_e \phi \bar{e}_L e_R + \text{h.c.}\right) + ... \end{aligned} \tag{2.21}$$

In the SM there are no right-handed neutrinos and the neutrinos are massless. We come back to this in the leptogenesis section.

Let's focus on the quarks. For three generations $u^i = (u, c, t)$ and $d^i = (d, s, b)$ and the yukawa matrices $Y_I$ with $I = u, d$ are general complex $3 \times 3$ matrices. We can diagonalize by a bi-unitary transformation

$$Y_I = U_I Y^{\rm D}_I W^\dagger_I, \quad I = u, d \tag{2.22}$$

with $U, W$ unitary matrices. Squaring we see that $Y_I Y^\dagger_I = U_I (Y^{\rm D}_I)^2 U^\dagger_I$, and $Y^{\rm D}_I$ are the positive square roots of this equation. The masses of the quarks can be made real by a chiral rotation; we will return to this in section 2.1.3. Now make the change of variables

$$u^i_R \to u^{i\prime}_R = W^{ij}_u u^i{}_R, \qquad u^i_L \to u^{i\prime}_L = U^{ij}_d u^i{}_L \tag{2.23}$$

and likewise for the $d$-fields. This transformation thus diagonalizes the quark mass matrix for the Lagrangian written in terms of the primed fields. The primed field are the mass eigenstates and the orginal fields are the flavor eigenstates. QCD, EM and the Z-interactions are diagonal in flavor space and do not mix $u_R$ and $d_R$, and also not $u_L$ and $d_L$. Rewriting the fermion currents in terms of the primed fields, only $W_I^\dagger W_I$-combinations appear and the $W_I$ rotating the right-handed fields drop out of the lagrangian. The $U_i$ rotating the left-handed fields likewise drop out, expcept for the charged current interactions which mix mix $u_L$ and $d_L$:

$$J^{\mu+} \supset \frac{1}{\sqrt{2}}\bar{u}_L\gamma^\mu d_L \to \frac{1}{\sqrt{2}}\bar{u}'_L\gamma^\mu(U_u^\dagger U_d)d'_L \equiv \frac{1}{\sqrt{2}}\bar{u}'_L\gamma^\mu V_{\rm CKM}d'_L \tag{2.24}$$

The CKM matrix $V_{\rm CKM} = U_u^\dagger U_d$ mixes different flavor states in the mass basis.

From now on we will work in the mass basis and drop the primes.

### 2.1.2 Sphalerons

The SM lagrangian is classically invariant under the global baryon and also under a global lepton U(1) symmetry. However, at the quantum level this symmetry is broken by the chiral anomaly, stemming from triangle diagrams, and the baryon current $J_B^\mu = \sum_q \frac{1}{3}\bar{q}\gamma^\mu q$ and lepton current $J_L^\mu = \sum_l(\bar{l}\gamma^\mu l + \bar{\nu}_l\gamma^\mu\nu_l)$ are non-conserved.

If we split the current in left- and right-handed pieces $\bar{f}\gamma_\mu f = \bar{f}_L\gamma_\mu f_L + \bar{f}_R\gamma_\mu f_R$ the non-conservation is

$$\partial^\mu \bar{f}_L\gamma_\mu f_L = -c_L\frac{g^2}{32\pi^2}F^a_{\mu\nu}\tilde{F}^{a\mu\nu}, \qquad \partial^\mu \bar{f}_R\gamma_\mu f_R = +c_R\frac{g^2}{32\pi^2}F^a_{\mu\nu}\tilde{F}^{a\mu\nu}, \tag{2.25}$$

with $F^{a\mu\nu}$ the field strength tensor and $\tilde{F}^{a\mu\nu} = \epsilon^{\mu\nu\alpha\beta}F^a_{\alpha\beta}/2$ the dual tensor. The constants $c_L, c_R$ depend on the representation of $f_L$ and $f_R$. The gauge group of the SM is is $SU(3)_c \times SU(2)_L \times U(1)_Y$. QCD is vector-like and both chiralities couple equally to the gluons, which gives $c_L^{QCD} = c_R^{QCD}$, and no anomaly. However the $SU(2)$ gauge fields only couple to left-handed fermions, and hypercharges differs for both chiralities, giving $c_R^W = 0$ and $c_L^Y \neq c_R^Y$. The result is

$$\partial^\mu J^B_\mu = \partial^\mu J^L_\mu = \frac{n_F}{32\pi^2}(g^2 W^a_{\mu\nu}\tilde{W}^{a\mu\nu} - g'^2 B_{\mu\nu}\tilde{B}^{\mu\nu}), \tag{2.26}$$

with $W^a_{\mu\nu}$ and $B_{\mu\nu}$ ($g$ and $g'$) the $SU(2)_L$ and $U(1)_Y$ field strengths (gauge couplings), $\tilde{W}_{\mu\nu} = \frac{1}{2}\epsilon_{\mu\nu\rho\sigma}W^{\rho\sigma}$ the dual field strength, and $n_F = 3$ is the number of generations.

The right hand side of eq. (2.26) can be written as the divergence of a current $\partial J^B = n_F\partial_\mu K^\mu$ with

$$K^\mu = \frac{g^2}{32\pi^2}2\epsilon^{\mu\nu\alpha\beta}W^a_\nu(\partial_\alpha W^a_\beta + \frac{g_w}{3}\epsilon^{abc}W^b_\alpha W^c_\beta) - \frac{g'^2}{32\pi^2}\epsilon^{\mu\nu\alpha\beta}B_\nu B_{\alpha\beta}. \tag{2.27}$$

Although the r.h.s. is a total derivative it does not vanish for the non-abelian field strength. For the classical energy to vanish at infinity, the corresponding field strength should vanish. For hypercharge this givea $B_\mu = 0$ and it does not contribute; however for a non-abelian gauge field eq. (2.12) this gives $2\partial^\alpha W_a^\beta = g\epsilon_{abc} W^{b\alpha} W^{c\beta}$, which yields a non-zero contribution to $K^\mu$. The variation of the total baryon number $B = \int \mathrm{d}^3x\, J_B^0$ is

$$\frac{\Delta B}{n_f} = \int \mathrm{d}^3x K^0|_{t_i}^{t_f} = \int \mathrm{d}^4x(\partial_0 K^0 - \partial_i K^i) = \int \mathrm{d}^4x \partial_\mu K^\mu \equiv \Delta N_{\mathrm{CS}} \tag{2.28}$$

where the integration is over a cylinder with radius at spatial infinity and height from $t_i$ to $t_f$. In the 3rd step we used Gauss law. Since $\partial_\mu K^\mu$ is gauge invaraint we can choose a gauge in which the divergence of the spatial current vanishes, allowing to rewrite $\partial_0 K^0 \to \partial_\mu K^\mu$ in 4-vector form. $\Delta N_{\mathrm{CS}}$ is the Chern-Simons number.

Because of the non-trivial vacuum topology of $SU(2)$ the Chern-Simons number is an integer. The gauge field is a map from the physical space to the manifold of the gauge group. SU(2) and the boundary of 4D space compactified on ball both are 3-spheres, and the map can have nontrivial homotopy (characterized by the winding number).

In more detail: the ground state corresponds to a time-independent field configuration with vanishing energy density $W_{\mu\nu} = 0$, which means that the gauge field is a pure gauge. Let's work in temporal gauge which sets $W_0 = 0$. The temporal gauge is a partial gauge fixing condition, as time-independent gauge transformations $U(\mathbf{x})$ leave the gauge fixing condition $W_0 = 0$ fixed: $W_0 \to \frac{i}{g} U(\mathbf{x})\partial_0 U^{-1}(\mathbf{x}) = 0$. The vacuum is thus described by the time-independent pure gauge configuration $\mathbf{W}(\mathbf{x}) = (i/g)U(\mathbf{x})\nabla U(\mathbf{x})^{-1}$. We can make use of the remaining gauge freedom to impose at spatial infinity $|\mathbf{x}| \to \infty$ that $\mathbf{W} = 0$ by choosing $U = 1$. Spatial infinity with all points at infinity identified is equivalent to $S^3$. Hence, by imposing this last condition the gauge transformation $U(\mathbf{x})$ becomes a mapping from $S^3$ to the gauge group[2] $SU(2) \sim S^3$.

These mappings fall into homotopy classes categorized by integer winding numbers. Two mappings $\mathbf{x} \to U_1(\mathbf{x})$ and $\mathbf{x} \to U_2(\mathbf{x})$ belong to the same class if there exists a continuous transformation from $U_1(\mathbf{x})$ to $U_2(\mathbf{x})$, which correspond to small gauge transformations, ie gauge transformations that can be continuously deformed to the identity transformation. Mappings in different homotopy classes correspond to distinct vacua, which are related by a large gauge transformation. The general configuration of

[2]The most generic $2 \times 2$ unitary matrix with determinant equal to unity may be expressed as $a\,\mathbb{1} + ib_i\sigma^i$ with the condition $a^2 + |b|^2 = 1$. Therefore the topology is $SU(2) \sim S^3$.

$\Delta B = \Delta L = \pm 3$ (

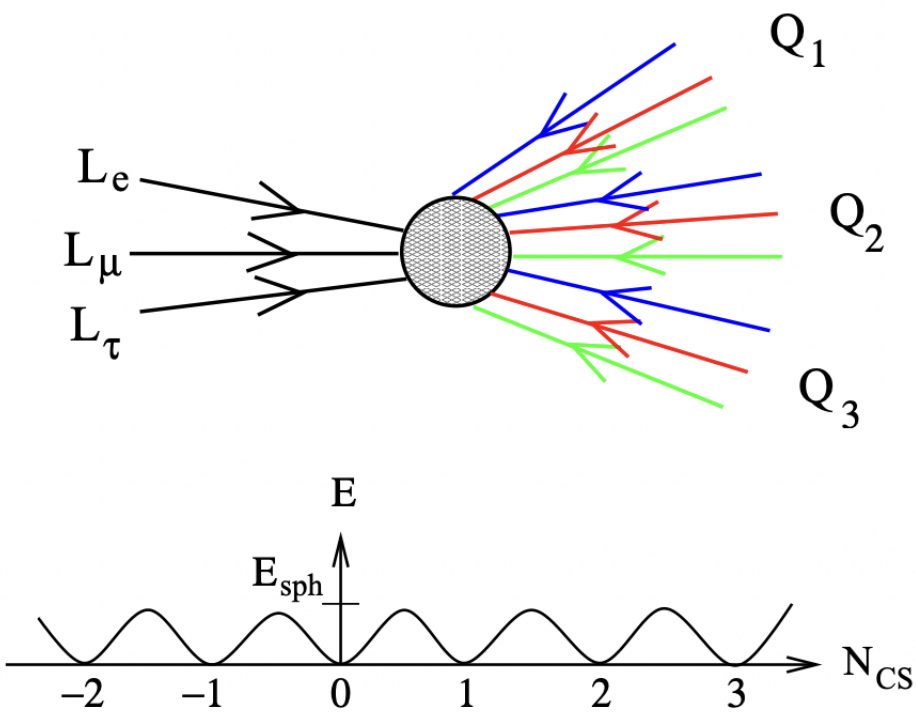


**Figure 1**. Sphalerons. Top: Feynman diagram for effective sphaleron interaction. Bottom: Energy of gauge field configurations as a function of Chern-Simons number. From [1].

the different vacua is given by (up to small gauge transformations)

$$U(\mathbf{x}) = \exp\left(\frac{i\pi\mathbf{x}\cdot\boldsymbol{\sigma}}{\sqrt{|\mathbf{x}|^2+\lambda^2}}n\right) \tag{2.29}$$

with $n = N_{\rm cs}$ the winding number, and $\lambda$ an arbitrary scale parameter.

As follows from eq. (2.26), in the SM the combination B-L is conserved $\partial^\mu(J^B_\mu - J^L_\mu) = 0$, while B+L is broken $\partial^\mu(J^B_\mu + J^L_\mu) \neq 0$. The different vacua of the theory are charachterized by the Chern-Simons number $N_{\rm CS}$. To transition between them costs a finite energy density, see the bottom plot in fig. 1. To find the height of the barrier between inequivalent vacua, one can construct the explicit solution that interpolates between the vacuum and the top of the barrier. This is the sphaleron solution, which is Greek for 'ready to fall', as the top of the barrier is an unstable state. The energy

of the sphaleron is found to be

$$E_{\rm sph} = f(\lambda/g)\frac{4\pi\phi}{g}, \quad f(\lambda/g) \sim 2. \tag{2.30}$$

with $\phi(T)$ the temperature dependent vev in the minimum.

At zero temperature the transition can only go via quantum mechanical tunneling, the tunneling action is non-perturbative and proportional to $g^{-2}$, and the rate is exceedingly small

$$\frac{\Gamma}{V} \sim {\rm e}^{-8\pi^2/g^2} \sim 10^{-185}. \tag{2.31}$$

This assures the stability of the proton. At finite temperature the thermal fluctuations may get the fields on top of the barrier, and it can then roll to the next vacuum. At high temperature $T \gtrsim m_W$ there is no barrier (before EW phase transition) and transitions are fast, on dimensional grounds

$$\frac{\Gamma_{\rm sph}}{V} \sim 10^{-6} T^4, \qquad T \gtrsim m_W \tag{2.32}$$

The constant of proportionality is found from lattice calculation, it is small as there is also dependence on the small gauge coupling. At lower temperatures the rate is Boltzmann suppressed by the energy of the sphaleron configuration, and

$$\frac{\Gamma_{\rm sph}}{V} \sim {\rm e}^{-E_{\rm sph}/T}, \qquad T \lesssim m_W \tag{2.33}$$

For rates exceeding the Hubble rate, $\Gamma > H$, the sphalerons are in thermal equilibrium. Taking $V \sim H^{-3}$ the Hubble volume, this gives

$$100\,{\rm GeV} \leq T \leq 10^{12}\,{\rm GeV} \tag{2.34}$$

The sphaleron transition violates baryon and lepton number by $\Delta B = \Delta L = \pm 3$, and involves quarks (with all colors) and leptons from all generations, see fig. 1 for the effective vertex interaction. An example $\Delta B = \Delta L = -3$ transition is

$$u + d \to \bar{d} + 2\bar{s} + \bar{c} + 2\bar{b} + \bar{t} + \bar{\nu}_e + \bar{\nu}_\mu + \bar{\nu}_\tau. \tag{2.35}$$

### 2.1.3 C and CP violation in the SM

The SU(2) gauge bosons only couple to left handed fermions, which breaks $C$ maximally. There are two source of CP violation in the SM, and the also the QCD phase transtion is a 2nd order transition.

The fermion masses can be complex. This breaks CP as the yukawas transform $Y \overset{\rm CP}{\to} Y^*$. However, these phases can be removed from the mass term by a global chiral

rotation of the fermions $f_L \to e^{i\alpha} f_L$ and $f_R \to e^{-i\alpha} f_R$. Via the chiral anomaly this generates a contribution to the QCD theta term[3]

$$\mathcal{L} \supset \bar{\theta} \frac{g^2}{32\pi^2} F_{\mu\nu} \tilde{F}^{\mu\nu}, \quad \bar{\theta} = \theta - \arg\det(Y_u Y_d) \tag{2.36}$$

$\tilde{F}^{\mu\nu} \sim E \cdot B$ violates CP. The $\bar{\theta}$ term gives rise to a non-zero electric dipole moment of the neutron $d_N = 5.2 \times 10^{-16} \bar{\theta}\, \mathrm{e} \cdot \mathrm{cm} < 10^{-26}\, \mathrm{e} \cdot \mathrm{cm}$. Hence $\bar{\theta} < 10^{-10}$ is too small for baryogenesis.

The second source of CP violation is the CKM matrix, if $V_{\mathrm{CKM}}$ contains phases

$$\bar{u}_L \gamma^\mu V_{\mathrm{CKM}} W^{-\mu} d_L + \bar{d}_L \gamma^\mu V^*_{\mathrm{CKM}} W^{+\mu} u_L \overset{\mathrm{CP}}{\to} \bar{d}_L \gamma^\mu V_{\mathrm{CKM}} W^{+\mu} u_L + \bar{u}_L \gamma^\mu V^*_{\mathrm{CKM}} W^{-\mu} d_L \tag{2.37}$$

The number of parameters in the $3 \times 3$ unitary matrix $V_{\mathrm{CKM}}$ is $2 \times 3^2$ minus $3^2$ real conditions from the unitarity constraint, giving 9 real parameters. Three of those are mixing angles, the number of parameters of a $O(3)$ rotation, and there are 6 phases. We can remove phases by a rotation of the quark fields

$$u^i_L \to \mathrm{e}^{i\alpha^i} u^i_L, \quad d^i_L \to \mathrm{e}^{i\alpha^i} d^i_L \tag{2.38}$$

The overall phase is redundant, and this removes 5 phases.

The CKM matrix thus contains one phase, which breaks CP. Commonly the Wolfenstein parameterization is used for the CKM matrix, but where the phase resides can be changed by field rotations. It follows that all three generations should be involved in a process for CP to be violated (for two quarks the $2 \times 2$ CKM matrix has no phase). An invariant way to parameterize CP violation is the Jarlskog invariant $J = \det[m_u^2, m_d^2]$ with the masses in the flavor basis (before diagonalizing the mass matrix); this parameterization is invariant under rotations of the fields. This gives

$$J_{\mathrm{CP}} = \prod_{\substack{i>j \\ u,c,t}} (m_i^2 - m_j^2) \prod_{\substack{i>j \\ d,s,b}} (m_i^2 - m_j^2)\, \mathrm{Im}(V_{ud} V_{cb} V^*_{ub} V^*_{cd}), \tag{2.39}$$

Inserting the measured CKM matrix elements gives $\mathrm{Im}\,(V_{ud} V_{cb} V^*_{ub} V^*_{cd}) \simeq 2 \times 10^{-5} \sin\delta_{KM}$. To get a dimensionless measure of the CP asymmetry, we can divide it by $T^{12}_{\mathrm{EW}}$, as the EW temperature is the lowest scales where sphaleron transitions occur. This gives

$$\frac{J_{\mathrm{CP}}}{(100\,\mathrm{GeV})^{12}} \sim 10^{-20} \tag{2.40}$$

which is too small for baryogenesis.

[3]No theta term is generated for the SU(2) gauge fields, as they only couple to left-handed fields, and thus we have the freedom to use rotation of the right-handed fields to remove phases in the mass matrix.

### 2.1.4 Non-equilibrium processes in the SM

We can be short. Starting with a universe at high temperature, within the SM there are no sources for much out of equilibrium physics. The EW phase transition is a smooth cross over.

## 3 Leptogenesis

In the SM the neutrinos are massless. We now know from oscillation experiments that neutrinos have a mass. We can give a dirac mass to the neutrinos by adding (three) right handed neutrinos (RHNs). The RHN are singlets under the SM gauge symmetries, and therefore they can be majorana fermions, that is, they can be their own antiparticle. This also allows to add an extra majorana mass coupling the RHNs. This is the (type I) seesaw mechanism for neutrino masses, where the mass eigenstates of the light active neutrinos are suppressed by the heavy mass scale of the RHN.

The majorana mass term breaks lepton number. A non-zero lepton number will be reprocessed by the equilibrium $B-L$ conserving sphaleron transtions in a non-zero baryon number. In the vanilla scenario, the lepton number is generated by the out of equilibrium decay of the (lightest) right-handed neutrino. There can be CP violating phases in the additional couplings in the Lagrangian involving the RHNs. Then the decay of the RHN into leptons and into anti-leptons may differ $\Gamma(N \to lH) \neq \Gamma(N \to \bar{l}\bar{H})$.

### 3.1 Neutrino mass

The Dirac mass couples left and right chiralities, whereas a majorana mass couples right with right (or left with left). The terms in the lagrangian and the mass matrix is most easily written down in terms of the neutrinos and their charge conjugates. A Dirac neutrino transforms under charge conjugation as eq. (2.2)

$$C\psi C^{-1} = -i\gamma^2\psi^* = -i\gamma^2\gamma^0(\psi^\dagger\gamma^0)^T = -i\gamma^2\gamma^0\bar{\psi}^T \tag{3.1}$$

Applying charge conjugate twice gives back the original spinor $(\psi^c)^c = -i\gamma^2(-i\gamma^2\psi^*)^* = \psi$. The chirality of $\psi^c$ is the opposite of the chirality $\psi$

$$\gamma^5\psi^c = \gamma^5(-i\gamma^2\gamma^0\bar{\psi}^T) = -i\gamma^5\gamma^2\psi^* = i\gamma^2\gamma^5\psi^* = -(\gamma^5\psi)^c \tag{3.2}$$

Thus the charge conjugate of a left-handed field is a right handed field and vice versa. We can see this explicitly. Use the notation for a left and right handed neutrino

$$\nu_L = \begin{pmatrix} \psi_L \\ 0 \end{pmatrix}, \quad \nu_R = \begin{pmatrix} 0 \\ \psi_R \end{pmatrix}, \tag{3.3}$$

then under charge conjugation

$$\nu_L \xrightarrow{\mathcal{C}} \nu_L^c = \begin{pmatrix} 0 \\ (i\sigma^2\psi_L^*) \end{pmatrix}, \qquad \nu_R \xrightarrow{\mathcal{C}} \nu_R^c = \begin{pmatrix} (-i\sigma^2\psi_R^*) \\ 0 \end{pmatrix} \tag{3.4}$$

Thus $\nu_L$ and $\nu_R^c$ are lefthanded, and $\nu_R$ and $\nu_L^c$ right-handed.

Let's now write down the Dirac mass for the neutrinos. For a real Dirac mass we can write it in terms of the Dirac spinor $\psi = \nu_L + \nu_R$ as $m_D\bar{\psi}\psi = m_D\bar{\nu}_L\nu_R + \text{h.c.}$. For a complex mass term we can start from the 2nd definition, in terms of the chiral fields, which is general. The Dirac mass term thus is[4]

$$\begin{aligned} \mathcal{L}_{\text{Dirac}} &= -m_D\bar{\nu}_L\nu_R + \text{h.c.} = -\big(\frac{1}{2}m_D\bar{\nu}_L\nu_R + \frac{1}{2}m_D^T\overline{\nu_R^c}\nu_L^c + \text{h.c.}\big) \\ &= -\frac{1}{2}\begin{pmatrix}\overline{\nu_L^c} & \overline{\nu_R}\end{pmatrix}\begin{pmatrix} 0 & m_D^T \\ m_D & 0 \end{pmatrix}\begin{pmatrix}\nu_L \\ \nu_R^c\end{pmatrix} + \text{h.c.} \end{aligned} \tag{3.6}$$

Likewise we can write down a majorana mass term for the real majorana spinor $\psi = \nu_R + \nu_R^c$ as $m_M\bar{\psi}\psi = m_M\overline{\nu_R^c}\nu_R + \text{h.c.}$ and

$$\mathcal{L}_{\text{Majorana}} = -\frac{1}{2}m_R\overline{\nu_R^c}\nu_R + \text{h.c.} = -\frac{1}{2}\begin{pmatrix}\overline{\nu_L^c} & \overline{\nu_R}\end{pmatrix}\begin{pmatrix} 0 & 0 \\ 0 & m_R \end{pmatrix}\begin{pmatrix}\nu_L \\ \nu_R^c\end{pmatrix} + \text{h.c.} \tag{3.7}$$

In the SM a majorana mass term for the left-handed neutrino, which is a part of an SU(2) doublet, is forbidden by gauge symmetry.

A global U(1) lepton number transformation $\nu_I \to \mathrm{e}^{i\alpha}\nu_I$ with $I = L, R$ leaves the Dirac mass is invariant at the classical level. As $\overline{\nu_R^c} \to \mathrm{e}^{i\alpha}\overline{\nu_R^c}$ the majorana mass term breaks lepton number explicitly $\mathcal{L}_{\text{Majorana}} \to \mathrm{e}^{2i\alpha}\mathcal{L}_{\text{Majorana}}$ by $\Delta L = 2$.

Adding dirac and majorana mass the mass matrix is

$$\mathcal{L}_{\text{mass}} = -\bar{\psi}_L M\psi_R + \text{h.c.}, \quad M = \begin{pmatrix} 0 & m_D \\ m_D^T & m_R \end{pmatrix} \tag{3.8}$$

with $\psi_L = (\nu_L\ \nu_R^c)^T$ and $\psi_R = (\nu_L^c\ \nu_R)^T$. A generic non-hermitian matrix can by diagonalized by a bi-unitary transformation. For a symmetric matrix $M^T = M$ we get the relation

$$M_D = V^\dagger M U \quad \Rightarrow \quad M_D = M_D^T = U^T M^T V^* = U^T M V^* \quad \Rightarrow \quad U = V^* \tag{3.9}$$

[4]The relation $m_D\bar{\nu}_L\nu_R = m_D^T\bar{\nu}_R^c\nu_L$ follows from

$$m\bar{\psi}\chi^c = m\psi^\dagger\gamma^0(-i\gamma^2\chi^*) = -im(\psi^*)^T\gamma^0\gamma^2\chi^* = im(\psi^*)^T\gamma^2\gamma^0\chi^* = -im^T\chi^\dagger\gamma^0\gamma^2\psi^* = m^T\bar{\chi}\psi^c. \tag{3.5}$$

with $M_D$ a diagonal matrix. To diagonalize the mass matrix we thus use

$$M_D = U^\dagger M U^* \tag{3.10}$$

If there is a hierarchy between the mass scale of the dirac mass and the majorana masses, the off-diagonal mixing is suppressed and we can expand in small mixing angle.[5]

We will eventually consider the implementation in the SM with three generations of left-handed and $n_R$ right-handed neutrinos, but let's for now take a single generation. Then for small mixing

$$U \approx \begin{pmatrix} 1 & \theta \\ -\theta^\dagger & 1 \end{pmatrix}, \quad U^\dagger M U^* = \begin{pmatrix} -\theta m_D^T - m_D\theta^T + \theta m_R \theta^T & m_D - \theta m_R \\ m_D^T - m_R\theta^T & m_R \end{pmatrix} \tag{3.12}$$

up to higher order $\theta$-corrections. Demanding the off-diagonals to vanish gives the angle in the mixing matrix

$$\theta = m_D m_R^{-1} \tag{3.13}$$

The light neutrino (upper left corner) and heavy neutrino (lower right corner) masses are

$$m_\eta \approx -m_D m_R^{-1} m_D^T = -\theta m_R \theta^T, \quad m_N \approx m_R \tag{3.14}$$

The mass eigenstates are majorana fermions. The rotated fields are $\phi_R = U^T \psi_R$ and $\phi_L = U^\dagger \psi_L$, and the mass eigenstates can be written as (we take $\theta$ real, as is the case for the one generation case)

$$\begin{aligned} \eta &= \eta_L + \eta_R = \nu_L + \nu_L^c - \theta(\nu_R + \nu_R^c) = \eta^c, \\ N &= N_L + N_R = \nu_R + \nu_R^c + \theta(\nu_L + \nu_L^c) = N^c \end{aligned} \tag{3.15}$$

As expected the light mass eigenstate is mostly the left handed state $\eta_L \approx \nu_L$ that enters in the weak interaction, and $N_R$ is mostly the inert $\nu_R$ state.

### 3.2 SM with right-handed netrinos

Add $n_R$ right-handed neutrinos to the SM Lagrangian eq. (2.13), with both a Dirac and Majorana mass. The lepton sector of the Lagrangian is

$$\begin{aligned} \mathcal{L} \supset\ & \bar{l}_L i\not{D}\, l_L + \bar{e}_R i\not{D}\, e_R + \frac{1}{2}\bar{\nu}_R i\not{\partial}\, \nu_R - (\bar{l}_L Y_e H\, e_R + \bar{l}_L Y_\nu \tilde{H}\, \nu_R + \frac{1}{2} m_R \overline{\nu_R^c} \nu_R + \text{h.c.}) \\ =\ & \frac{g}{\sqrt{2}} \left( W_\mu^+ J_{W^+}^\mu + \text{h.c.} \right) + \frac{g}{\cos^2\theta_W} Z_\mu J_Z^\mu - (\bar{e}_L Y_e \phi\, e_R + \bar{\nu}_L Y_\nu \phi\, \nu_R + \frac{1}{2} m_R \overline{\nu_R^c} \nu_R + \text{h.c.}) + ... \end{aligned} \tag{3.16}$$

[5] A general unitary matrix is of the form

$$U = \begin{pmatrix} a & b \\ -b^\dagger & a^\dagger \end{pmatrix}, \quad |a|^2 + |b|^2 = 1 \tag{3.11}$$

Without loss of generality we can work in a basis in which $m_R$ is diagonal. One can always diagonalize the $3 \times 3$ charged lepton yukawa mass matrix $m_D^e = Y_e \phi/\sqrt{2}$ via a bi-unitary transformation $l_L = U^l \tilde{l}_L$ and $l_R = V^l \tilde{l}_R$. The neutral current is invariant but the charged current transforms, and $U_l$ appears in the Lagrangian in the following terms

$$\mathcal{L} \supset -\frac{g}{\sqrt{2}} \bar{\nu}_L \gamma^\mu U_l \tilde{e}_L W_\mu^+ - \bar{\nu}_L m_D \tilde{\nu}_R + \text{h.c.} \tag{3.17}$$

We can define $\tilde{\nu}_l = U_l \tilde{\nu}_l$ and $\tilde{m}_D = U_l m_D$ to remove $U_l$ from the lagrangian. This is weak interaction basis. In this basis the charged current interaction produces a charged lepton mass eigenstate $\tilde{e}_l$, together with a neutrino $\tilde{\nu}_L$ which is a weak interaction eigenstate. From now on we work in the weak interaction basis, and we drop the tildes.

The neutrino mass matrix is of the form eq. (3.8), with now the Dirac mass $m_D = Y_\nu \phi/\sqrt{2}$ is $3 \times n_R$ dimensional, and the majorana mass $n_R \times n_R$. It can be diagonalized eq. (3.10) by the matrix

$$U = V_{\text{block}} \cdot V_{\text{light}} = \begin{pmatrix} 1 & \theta \\ -\theta^\dagger & 1 \end{pmatrix} \begin{pmatrix} U_\eta & 0 \\ 0 & 1 \end{pmatrix} \tag{3.18}$$

$V_{\text{block}}$ block diagonalizes the mass matrix in diagonal heavy and light blocks, and $V_{\text{light}}$ diagonalizes the light mass matrix

$$U_\eta^\dagger m_\eta U_\eta^* = m_\eta^{\text{diag}}, \tag{3.19}$$

with $m_\eta$ in eq. (3.14). Note that the light mass and flavor eigenstates are related $\nu_L = U_\eta \eta_L$ and $U_\eta$ is the PMNS matrix, which is the equivalent of the CKM matrix (the mixing matrix in the charged current interactions) in the lepton sector. This is in the weak interaction basis, where the charged lepton mass and flavor states are aligned.

### 3.3 Sakharov conditions in leptogenesis

Consider there RHNs with mass ordering $M_1 < M_2 < M_3$. Any asymmetry produced by the out of equilibrium decay of the heavier RHNs will be erased as the lightest state is still in equilibrium. We are thus interested in the out of equilibrium decay of the lightest $N_1 \approx \nu_{R1} + \nu_{R1}^c$ state.

**Lepton number violation** The majorana mass term for the RHNs breaks lepton number by $\Delta L = 2$. A non-zero initial lepton number $L_i$ is produced in the decay of the RHN. Sphaleron transitions (approximately) wipe out $B + L$ and conserve $B - L$: $(B + L)_f \approx 0$[6] and $(B - L)_f = (B - L)_i = -L_I$, which gives $B_f = -L_f = -\frac{1}{2} L_i$. A

[6]Only left-handed part of $B - L$ is erased by sphalerons, not the contribution of the right-handed particles.

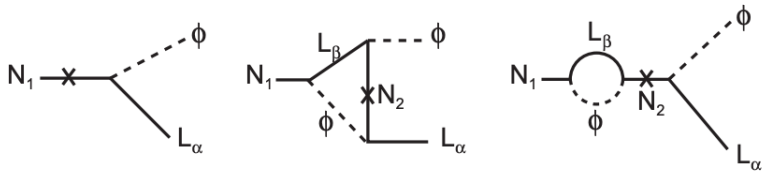


**Figure 2**. The diagrams contributing to the CP asymmetry $\epsilon$.

more carefull treatment, taking into account all reactions in thermal equilibrium and all conserved charges (e.g. hypercharge) gives $B_f = c(B-L)_i$ and $L_f = (c-1)(B-L)_i$ with

$$c = \frac{8N_f + 4N_H}{22N_f + 13N_H} \tag{3.20}$$

which gives $c = 0.35$ in the SM.

**CP violation** The decay of $N_1$ into leptons and antileptons is different in the presence of CP asymmetry, which we can parameterize by

$$\epsilon = \frac{\Gamma(N_1 \to lH) - \Gamma(N_1 \to \bar{l}H^*)}{\Gamma(N_1 \to lH) + \Gamma(N_1 \to \bar{l}H^*)} \tag{3.21}$$

At tree level, both decays in the nominator are proportional to $|\mathcal{M}|^2 \propto |Y_{1\alpha}|^2$ and cancel. Explicity

$$\Gamma_1 = \sum_\alpha \left[\Gamma(N_1 \to l_\alpha H) + \Gamma(N_1 \to \bar{l}_\alpha H^*)\right] = \frac{1}{8\pi} M_1 (Y^\dagger Y)_{ii} \tag{3.22}$$

CP violation arises from the interference of tree level and one-loop diagrams. We sketch here the calculation. Separate the tree and loop amplitudes in a coupling and a matrix part

$$\mathcal{M} = \mathcal{M}_0 + \mathcal{M}_1 = c_0 \mathcal{A}_0 + c_1 \mathcal{A}_1 \tag{3.23}$$

For the tree level part $c_0 = Y^*_{\alpha_1}$ and $\mathcal{A} = \bar{u}_{l_\alpha} P_R u_N$. The CP conjugate matrix is $\mathcal{M}_i = c_i^* \bar{\mathcal{A}}_i$, where in the conjugate amplitude $u$ spinors are replaced by $v$ spinors. Since only the momentum part of $\bar{u}u = \bar{v}v \to \not{p}$ survives the traces in the cross section calculation, we can effectively set $\bar{\mathcal{A}}_i = A_i$. The denominator in eq. (3.21) is dominated by the tree level decay, the nominator comes from the interference term

$$|\mathcal{M}|^2 + |\bar{\mathcal{M}}|^2 \approx 2|c_0|^2 |\mathcal{A}_0|^2. \quad |\mathcal{M}|^2 - |\bar{\mathcal{M}}|^2 = 4\mathrm{Im}(c_0 c_1^*)\mathrm{Im}(\mathcal{A}_0 \mathcal{A}_1^*). \tag{3.24}$$

The first factor contains phases in the couplings that violate C and CP. However, we also see that a CP conserving phase is needed in $\mathrm{Im}(\mathcal{A}_0\mathcal{A}_1^*)$, which can arise when the intermediate particles $H, l$ are on shell ($N_2$ is too heavy to be on-shell) in the loop diagrams. This follows from the unitarity of the S-matrix and the optical theorem. The $S$ matrix and amplitude are defined

$$\langle f|S|i\rangle = \langle f|1 - iT|i\rangle = S_{fi}, \quad \langle f|T|i\rangle = \mathcal{M}(i \to f), \tag{3.25}$$

with $i, f$ denoting initial and final states. Unitarity $S^\dagger S = 1$ implies $i(T - T^\dagger) = T^\dagger T$. This gives the relation

$$i\left[\mathcal{M}(i \to f) - \mathcal{M}^*(f \to i)\right] = \sum_n \langle f|T^\dagger|n\rangle\langle n|T|i\rangle \tag{3.26}$$

with the sum over all intermediate states. We can identify $i = N_i$ and $f = l_\alpha H$. In the limit of real couplings the lhs is proportional to $\mathrm{Im}(\mathcal{A}_1)$. The rhs shows the phase arises from intermediate states $n = l_\beta H, \bar{l}_\beta H^*$ going on-shell. This gives

$$2\mathrm{Im}(\mathcal{A}_0\mathcal{A}_1^*) = \mathcal{A}_0 \frac{\mathrm{d}^3 p_\beta}{2E_\beta(2\pi)^3}(2\pi)^4\delta^4(p_\beta - p_H^*)A_0^*(N \to \bar{l}'_\beta H^*)A_0^*(\bar{l}'_\beta H^* \to l_\alpha H) \tag{3.27}$$

In the limit that $M_j \gg M_1$ for $j = 2, 3$ one can approximate the propagator in $A_0^*(\bar{l}'_\beta H^* \to l_\alpha H)$. Explicit calculation gives

$$\epsilon_i \approx \frac{3}{4\pi}\frac{1}{(Y^\dagger Y)_{11}}\sum_\alpha \sum_{j=2,3} \mathrm{Im}\left[(Y^\dagger Y)_{1j}^2 Y_{\alpha j}\right]\frac{M_1}{M_j} \tag{3.28}$$

$\epsilon_i$ is zero for $i = j$, and we can extend the summation to $j = 1, 2, 3$. The coupling combination is genuinely CP violating if the phase cannot be removed by field redefinitions. We come back to this shortly.

The CP asymmetry is bounded from above, which for the hierarchical mass spectrum of $N_i$ can be derived as follows. We can write the phase factor in terms of the unit vector

$$\hat{Y}_\alpha = \frac{Y_{1\alpha^\dagger}}{\sqrt{(Y^\dagger Y)_{11}}} \tag{3.29}$$

and the neutrino mass matrix $(m_\eta)_{\beta\alpha} = \sum_j Y_{\beta j}^T Y_{\alpha j} v^2/M_j$ as proportional to $\propto \mathrm{Im}(\hat{Y}^T m_\eta \hat{Y})$. The neutrino mass matrix can be diagonalized by a bi-unitary transformation as in eq. (3.19) $U_\eta^\dagger m_\eta Y_\eta^* = m_\eta^{\mathrm{diag}}$. We can then rewrite

$$\epsilon_1 \propto \mathrm{Im}(\hat{Y}^T m_\eta \hat{Y}) = \mathrm{Im}(\hat{Y}^T U_\eta^* U_\eta^T m_\eta U U^\dagger \hat{Y}) = \mathrm{Im}(\hat{Y'}^T m_\eta^{\mathrm{diag}} \hat{Y'}) = \sum_\alpha \mathrm{Im}(\hat{Y'}_\alpha^2 m_\alpha) \leq m_{\max} \tag{3.30}$$

with $\hat{Y}' = U^\dagger Y$ and $m_{\rm max}$ is the heaviest light neutrino mass. This gives the upper bound on $|\epsilon|$, or equivalently lower bound on $M_1$

$$|\epsilon| \lesssim \frac{3M_1 m_{\rm max}}{16\pi v^2} \quad \Rightarrow \quad M_1 \gtrsim 10^9\,{\rm GeV} \left(\frac{m_{\rm atm}}{m_{\rm max}}\right)\left(\frac{|\epsilon|}{10^{-7}}\right) \tag{3.31}$$

Let's end this discussion with a counting of the invariant phases in the neutrino sector. Consider the lagrangian for neutino masses in the weak interaction basis and with diagonal right-handed neutrino masses. The yukawa coupling/Dirac mass is a general $3 \times n_R$ complex matrix with $3 \times n_R$ complex parameters; the majorana mass is diagonal and real and contains $n_R$ real parameters corresponding to the RHN masses. Three phases can be absorbed rotating $\nu_L$, but since $\nu_R$ is majorana they cannot be rotated. The lagrangian thus contains $2 \times 3 \times n_R + n_R - 3 = 7n_R - 3$ real parameters, of which $3 \times n_R - 3 = 3(n_R - 1)$ are phases.

At low energies the RHN can be integrated out, and the neutrino mass matrix for the light neutrinos eq. (3.14) is symmetric. For three families, this has 6 complex parameters. After diagonalizing the mass matrix, there are then six phases in the PMNS matrix. Three phases can be absorbed by rotating charged leptons, (cannot rotate the majorana neutrinos), hence three physical phases. There are then three phases in the PMNS matrix (one dirac phase and two majorana), three mixing angles, and three masses. If $N_R = 2$ one of the neutrino masses is massless, and there is only one majorana phase.

For $n_R = 3$, in the high scale lagrangian there are 18 parameters of which 6 phases. At low scales there are 9 parameters of which 3 are phases. There are thus 9 parameters in the RH sector, these correspond to the 3 RHN masses, and 3 complex parameters in the Casas-Ibarra $R$ matrix which gives the mixing between the light and heavy sector. Note that only 2 mass differences and 3 mixing angles are measured, hence there are many free parameters, making a general leptogenesis analysis difficult.

For $n_R = 2$, in the high scale lagrangian there are 11 parameters of which 3 phases. At low scales there are 7 parameters of which 2 are phases. There are thus 4 parameters in the RH sector, these correspond to the 2 RHN masses, and 1 complex parameters giving the mixing between the light and heavy sector.

We can measure all phases in the light neutrino sector, but in general there is no direct relation between these phases, and the phase that enters the lepton asymmetry parameter $\epsilon$ important for leptogenesis.

**Out of equilibrium** For a relativistic particle the equilibrium number density scales as $n \propto T^3$, while it is Boltzmann suppressed in the non-relativistic limit $n \propto {\rm e}^{-M_1/T}$. If the (inverse) decay rate is small the RHN cannot keep up with the equilibrium

density as the temperature drops below the mass, and the heavy neutrinos are not able to follow the rapid change of the equilibrium particle distribution. The decay is out of equilibrium; inverse decays are suppressed as the thermal bath particles have not enough energy to produce a RHN (except in the tail of the distribution). The out of equilibrium condition thus requires

$$K = \left.\frac{\Gamma_1}{H}\right|_{T=M_1} < 1 \tag{3.32}$$

with $\Gamma_1$ well approximated by the three level decay eq. (3.22).

Defining the effective neutrino mass scales

$$\tilde{m} = \frac{8\pi v^2}{M_1^2}\Gamma_1 = (Y^\dagger Y)_{ii}\frac{v^2}{M_1}, \quad m_* = \frac{8\pi v^2}{M_1^2}H(M_1) \approx 10^{-3}\,\text{eV} \tag{3.33}$$

then $K = \tilde{m}/m_*$. Here we used that $H(T) = \sqrt{\rho/(3M_{\rm P})} = \pi\sqrt{g_*}T^2/(3\sqrt{10}M_{\rm P})$ with $M_{\rm P} = 2.4 \times 10^{18}\,\text{GeV}$ the reduced planck mass. In the SM the number of relativistic degrees of freedom in the thermal bath at high temperature is $g_* = 106.75$. The effective neutrino mass $\tilde{m}$ is of the scale of the light neutrinos; one can show that the lightest neutrino mass $m_1 < \tilde{m}$.

### 3.4 Final baryon asymmetry

To calculate the lepton asymmetry one has to solve the Boltzmann equations for the densities of the RHNs and for the leptons. We will not do that here but estimate the result. The asymmetry depends on weather the out-of-equilibrium condition eq. (3.32) is satisfied or not.

Consider first the strong wash out regime $K \gg 1$. At $T \sim M_1$, a thermal number density of $N_1$ is obtained ($n_{N_1} \sim n_\gamma$) independent of the initial conditions. The total lepton number asymmetry at $T \sim M_1$ is effectively zero as any asymmetry made in the production of $N_1$ is washed out. The asymmetry in decay is washed out by inverse decays/scattering until these reaction at $T = T_F$ drop out of equilibrium. [7] At that time the remaining $N_1$ density is Boltzman suppressed $\propto \mathrm{e}^{-M_1/T_F} \approx K^{-1}$. We thus estimate the produced baryon asymmetry

$$Y_B \sim 0.35|Y_L| \sim 10^{-3}|\epsilon_1|K^{-1} \tag{3.34}$$

with $Y_i = n_i/s$. The equilibrium number density of $N_i$ divided by the entropy density, which gives a factor $n_{N_1}^{\rm eq}/s = 135\zeta(3)/(4\pi^4 g_\star) \approx 4 \times 10^{-3}$ for $g_* = 106.75$. This gives the overall coefficient above.

[7] At $T < M_1$ the rate for inverse decay is $\Gamma_{\rm ID} \approx \frac{1}{2}\Gamma_D \mathrm{e}^{-M_1/T}$.

In the weak washout regime $K < 1$ the total decay rate is small. The final lepton asymmetry now depends on the initial conditions. The "thermal leptogenesis" scenario assumes that the initial $N_1$ number density at high temperatures $T \gg M_1$ is zero. Both production and decay of RHN are mediated by the same Yukawa interactions, and if $\Gamma_D < H$ at $T = M_1$ then so is $\Gamma_{\rm prod} < H$. The RHN number density will not reach the thermal equilibrium distribution. Production is most efficient at $T \sim M_1$ at a time $t^* \sim 1/(2H(M_1))$ and the number density is $n_{N_1} \sim \Gamma_{\rm prod} t_U^* \sim n_\gamma K$. The lepton asymmetry produced in out of equilibrium production is partly depleted by scattering and (inverse) decays – not fully efficient, as it is out of equilibrium – and this avoids that any asymmetry generated in production of $N_1$ is subsequently erased by the out of equilibrium decay. This gives another $K$ suppression factor though. We thus estimate

$$Y_B \sim 0.35|Y_L| \sim 10^{-3}|\epsilon_1|K \qquad \text{for } n_{N_1}(T \gg M_1) \approx 0 \tag{3.35}$$

In both the weak and strong washout regime we need $|\epsilon_1| \gtrsim 10^{-7}$ to obtain the observed asymmetry. This implies large RHN masses $M_1 \gtrsim 10^9\,\text{GeV}$ eq. (3.31). Hence, we won't be able to probe the RHN in experiments. Neutrinoless double beta decay is only possible for a the mixing between the light and heavy light majorana neutrino, which hints to the seesaw mechanism with majorana RHN. If measures, this may be a hint but doen no prove that leptogenesis is responsible for the baryon asymmetry.

Note thoughtthat the lower bound on the RHN mass is derived for a hierarchichal spectrum $M_1 \ll M_2, M_3$. Al asymmetry is derived from the interaction of the lightest RHN. However, for a more dense mass spectrum, this will no longer be the case, and flavor effects and oscillations may become important. It is then possible to obtain the observed asymmetry for ligther RHN masses.

## 4 EW baryogenesis

At high temperature the EW sphalerons are in thermal equilibrium and any preexisting $B - L$ symmetry is washed out. In EW baryogenesis baryon number is generated at the electroweak phase transition. The picture is as follows:

The PT is first order and bubbles of true vacuum are nucleated, and expand into the surrounding plasma. The plasma particles scatter off the bubble wall, and if this interaction violates CP, the scattering is different for particles and antiparticles, which will then have different transmission and reflection coefficients. For example, the presence of the CP violating top yukawa coupling eq. (4.1), may lead to an overdensity of left-handed antiparticles over particles in front of the bubble wall (and a compensating overdensity of right-handed particles over antiparticles, as this interaction does not

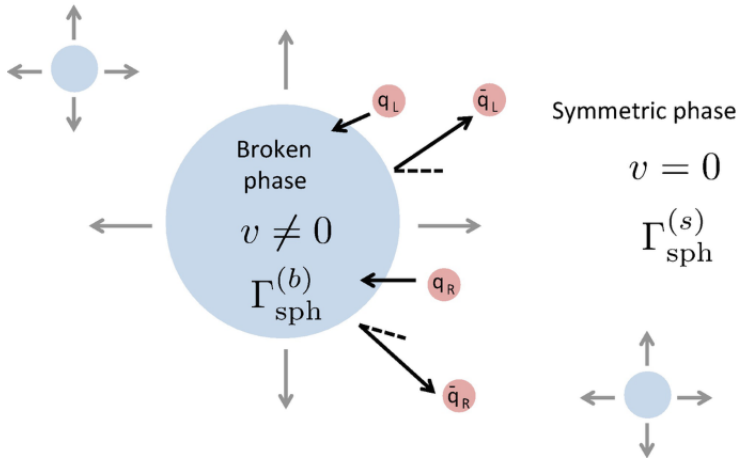


**Figure 3**. Electroweak baryogenesis mechanism.

violate baryon number). The EW sphaleron transition only interact with left-handed particles. As there is an overdensity of left-handed antiparticles this will bias the sphaleron rate which destroys antiparticles (in favor of particles as it violates baryon number) over the inverse rate, and a net baryon asymmetry is created.

Left to itself, all the fast plasma interactions would bring the system back to equilibrium, and erase the asymmetry. But there is not enough time for this to happen as the baryons are swept up by the expanding bubbles. If the PT is strong $v/T \gtrsim 1$ the sphaleron rate eq. (2.33) is suppressed inside the bubble, and the baryons remain. At the end of the PT, when bubbles collide and coalescence, there will be a net baryon number created.

Consider how the Sakharov conditions are satisfied in EWBG. Baryon number is violated by sphaleron transitions and C is maximally violated by the weak interactions. The CP violation in the SM is too small and new sources of CP are needed. For it to be important during the EWPT, this new physics should live around the TeV scale. As an example of a CP violating new coupling, consider the correction to the top quark yukawa interaction

$$\mathcal{L} \supset \frac{y_t}{\sqrt{2}}\phi\left(1 + c\frac{\phi^2}{\Lambda^2}\right)\bar{t}_L t_R + \text{h.c.} \tag{4.1}$$

with $\phi$ the radial higgs field. The dimension-6 operator can be thought of as generated from integrating out new physics at the scale $\Lambda$. If $\text{Im}(c) \neq 0$ then CP is violated. In the vacuum $\phi = v + h$, and the effective top mass is $m_t = \frac{y_t}{\sqrt{2}}v\left(1 + c\frac{v^2}{\Lambda^2}\right)$. The phase can be rotated away by a chiral transformation $t_L \to \mathrm{e}^{i\alpha}t_L$ and $t_R \to \mathrm{e}^{-i\alpha}t_R$. This is the standard procedure to make the mass matrix real. However, in the CP violating

bubble wall background the higgs field value $v(x)$ is space-time dependent, and cannot be rotated away by a global rotation. Hence the effective top mass in the bubble wall background is complex – in particular, inside the bubble wall where the vev changes – and the corresponding CP violation is physical and can generate an asymmetry between $t_L$ and $\bar{t}_L$. Note that in the vacuum the $\bar{t}th$-coupling still violates CP, which can be probed in e.g. electric dipole moment experiments.

A phase transition (PT) corresponds to a change of the physical state (phase) of a system due to changing external conditions (e.g. T, B,..) described in terms of an order parameter. The order parameter of the EWPT can be taken as the Higgs vev $\phi^2 = \langle H^\dagger H \rangle$ which breaks the EW symmetry $SU(2) \times Y(1)_Y \to U(1)_Q$.

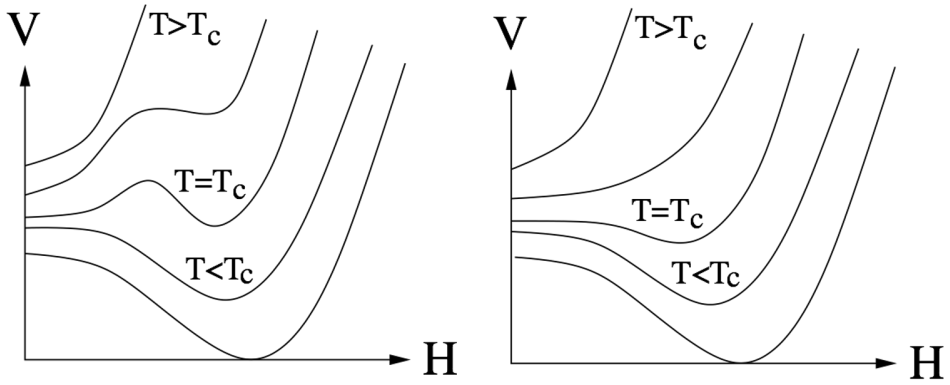


**Figure 4**. Potential for 1st and 2nd order/crossover PT. For 1st order PT the order parameter changes discontinuously, and PT proceeds via bubble nucleation.

The out of equilibrium dynamics requires the EW phase transition – in which the order parameter $\phi$ becomes non-zero and breaks the EW symmetry – is first order, and proceed via bubble nucleation. The EW potential at zero temperature is the Mexican hat potential. Calculating quantum corrections to the potential in the presence of a thermal bath (and not vacuum), the loop particles can exchange energy with the plasma (there are now quantum and thermal fluctuations), and the corrections become temperature dependent. At high temperature the dominant effect is a large effective temperature dependent mass term for the Higgs, and the minimum of the Higgs potential is at the origin; the electroweak symmetry is restored.

The order of the PT depends on the zero temperature potential and on thermal corrections. A 1st order PT arises if there is a barrier between the true and false vacuum, and the PT goes via tunneling and the nucleation of bubbles; otherwise the transition is a smooth 2nd order/cross over instead and the order parameter changes smoothly from its value in the false to that in the true vacuum everywhere in spacetime.

With the particle content of the SM the EWPT is a cross over. New physics in the Higgs sector is needed for a 1st order transition and for the EWBG scenario.

The EWBG requires new physics at the EW scale, which can be probed by colliders (e.g. by measuring the triple Higgs coupling), measurements of the electric dipole moment of the electron (which probes CP violation), and possibly in the future gravitational wave experiments (the colliding bubbles and the colliding sound waves in the plasma generate gravitational waves).

### 4.1 The Higgs potential at finite temperature

Further reading: book on thermal field theory [13], lecture notes on thermal field theory [7] and on on thermal field theory and the effective potential [8]. We will consider the one-loop corrections to the potential. The discussion on the SM in section 4.1.2 follows [1].

Goal: calculate the scalar potential $V(\phi_0, T)$ at finite temperature. The tree-level potential receives quantum corrections. In presence of a heat bath, loop particles can exchange energy-momentum with the bath, and the corrections become temperature dependent.

Work in the grand canonical ensemble: system can exchange energy, charge and particles with the heat reservoir, while temperature, volume and chemical potentials are kept fixed. For simplicity, set the chemical potentials to zero. The state of the system is described by the density operator $\rho$. The partition function is defined as the trace over the density operator (units $k_B = 1$)

$$Z = \mathrm{tr}\rho = \mathrm{tr}(\mathrm{e}^{-\beta H}), \quad \beta = 1/T \tag{4.2}$$

All thermodynamic quantities can be derived from the partition function, e.g. the pressure is $P = T(\partial \ln Z)/(\partial \mathcal{V})$. We are interested in the free energy density $F = -T \ln Z$, which is minimized in equilibrium, and can be interpreted in a constant background as the effective potential: $V_{\text{eff}} = F/\mathcal{V}$ with $\mathcal{V}$ the volume.

If we compare the density operator $\rho = \mathrm{e}^{-\beta H}$ with the the time-evolution operator $U(t) = \mathrm{e}^{-iHt}$, then we can see that that $-i\beta$ plays the role of time variable. Define the imaginary time variable

$$\tau = it, \quad 0 < \tau < \beta = 1/T \tag{4.3}$$

This observation underlies the statement that the finite temperature equilibrium field theory is equivalent to the Euclidean theory defined on a finite imaginary 'time' interval. Many methods developed for the description of zero-temperature quantum field theory can be generalized to the non-zero temperature case.

In QFT the generating function can be expressed in terms of the time evolution operator, which leads to the path integral formulation

$$Z = \int \mathrm{d}\phi_i \mathrm{d}\phi_f \langle \phi_f(\mathbf{x}, T)|U(\mathcal{T})|\phi_i(\mathbf{x}, 0)\rangle = \int \mathcal{D}\phi \, \mathrm{e}^{i\int_0^T \mathrm{d}^4x \mathcal{L}(\phi)} \tag{4.4}$$

with boundary conditions $\phi(0) = \phi_i$ and $\phi(\mathcal{T}) = \phi_f$ (here the wave functions $\langle 0|\phi_f\rangle\langle\phi_i|0\rangle$ are surpressed, as is usually done, as they constitute an irrelevant normalization factor). The path integral runs along the contour $\mathcal{C}$ that spans from $0 < t < \mathcal{T}$. The finite temperature partition function is obtained from this by Wick rotating to euclidean time, and compactifying the Euclidean time direction

$$Z = \mathrm{tr}(\rho) = \int \mathrm{d}\phi \, \langle\phi|\mathrm{e}^{-\beta H}|\phi\rangle = \int \mathcal{D}\phi \, \mathrm{e}^{-\int_0^\beta \mathrm{d}\tau \int \mathrm{d}^3x \mathcal{L}_E} \tag{4.5}$$

with (anti) periodic boundary conditions $\phi(0) = \pm\phi(\beta)$ for bosons (fermions), and with $\mathcal{L}_E = -\mathcal{L}(t \to \tau = it)$ the Euclidean action. The path integral contour $\mathcal{C}$ now spans from $0 < \tau < \beta$. As the fields are (anti)-periodic in imaginary time, they can be expanded in a Fourier series

$$\phi(\mathbf{x}, \tau) = \sum_n \phi(\mathbf{x}, \omega_n)\mathrm{e}^{i\omega_n\tau}, \quad \omega_n = \begin{cases} \frac{2\pi n}{\beta}, & \text{bosons,} \\ \frac{2\pi(n+1)}{\beta}, & \text{fermions.} \end{cases} \tag{4.6}$$

with Matsubara frequencies $\omega_n$. The compactness of the time interval makes the energy variable discrete.

### 4.1.1 Thermal corrections to the potential

The goal is to calculate the one-loop potential in field theory at finite temperare. This can be derived from the free (quadratic) Lagrangian, which itself can be viewed as a collection of harmonic oscillators, one for each momentum mode $\mathbf{k}$. Let's thus start with quantum mechanics and the harmonic oscillator first.

The Euclidean version of the generating function is

$$Z = \int \mathrm{d}q_f \mathrm{d}q_i \, \langle q_f|\mathrm{e}^{-H\mathcal{T}}|q_i\rangle = \int [\mathrm{d}q]\mathrm{e}^{-S_E}, \tag{4.7}$$

We are interested in the free energy $F = -\frac{1}{\mathcal{T}}\ln Z$ of the system, and we can be cavalier with the normalization factors of $Z$. We will work with the middle expression, but same results can be derived from the path integral formulation. The Hamiltonian for the harmonic oscillator is $H = \omega(N + \frac{1}{2})$, and $H|n\rangle = E_n|n\rangle = \omega(n + \frac{1}{2})|n\rangle$. Then eq. (4.7) gives

$$Z = \langle q_f|\mathrm{e}^{-HT}|q_i\rangle = \sum_n \mathrm{e}^{-E_nT} \int \mathrm{d}q_f \mathrm{d}q_i \, \langle q_f|n\rangle\langle n|q_i\rangle, \qquad F = \lim_{T\to\infty}(-\frac{1}{T}\ln Z) = \frac{1}{2}\omega \tag{4.8}$$

In the limit of euclidean time $\mathcal{T} \to \infty$ the free energy $F$ is dominated by the lowest lying energy state with $n = 0$ and F=$E_0 = \frac{1}{2}\omega$.

Now consider the harmonic oscillator at finite temperature. Wick rotate to euclidean time and take the interval $0 \leq \tau = it \leq \beta$ compact. The partition function is

$$Z = \int \mathrm{d}q \, \langle q|\mathrm{e}^{-H\beta}|q\rangle \sim \sum_n \mathrm{e}^{-\beta\omega(n+\frac{1}{2})}\langle n|q\rangle\langle q|n\rangle \sim \frac{\mathrm{e}^{-\beta\omega/2}}{1-\mathrm{e}^{-\beta\omega}},$$
$$F = \frac{1}{2}\omega + T\ln(1-\mathrm{e}^{-\beta\omega}) \tag{4.9}$$

where we used $F = -1/\beta \ln Z$. The first term is the zero temperature contribution, same as we found before eq. (4.8).

The fermionic harmonic oscillator has energy $E_n|n\rangle = \omega(n - \frac{1}{2})$, and the Hilbert space only contains two states $n = 0, 1$ due the Pauli exclusion principle. In this case the free energy is

$$Z = \int \mathrm{d}q \, \langle q|\mathrm{e}^{-H\beta}|q\rangle \sim \sum_{n=0,1} \mathrm{e}^{-\beta\omega(n-\frac{1}{2})}\langle n|q\rangle\langle q|n\rangle \sim \mathrm{e}^{\beta\omega/2}(1+\mathrm{e}^{-\beta\omega})$$
$$F = -\frac{1}{2}\omega - T\ln(1+\mathrm{e}^{-\beta\omega}) \tag{4.10}$$

A free quantum field can be viewed as a collection of harmonic oscillators, one for each frequency $\mathbf{k}$. This can be made precise by putting the field in a finite volume, which gives discretized momenta. The (leading one-loop) correction to the potential $V^{(1)}$ is thus given by the momentum integral of eqs. (4.9) and (4.10) with frequency $\omega_k = \sqrt{\mathbf{k}^2 + m^2}$, which gives

$$V^{(1)} = \sum_{\text{bosons}} n_i \int \frac{\mathrm{d}^3\mathbf{k}}{(2\pi)^3}\left(\frac{1}{2}\omega_i + T\ln(1-\mathrm{e}^{-\beta\omega_i})\right) - \sum_{\text{fermions}} n_i \int \frac{\mathrm{d}^3\mathbf{k}}{(2\pi)^3}\left(\frac{1}{2}\omega_i + T\ln(1+\mathrm{e}^{-\beta\omega_i})\right) \tag{4.11}$$

with $\omega_i = \sqrt{\mathbf{k}^2 + m_i(\phi)^2}$ and $n_i$ the degrees of freedom, e.g. for a dirac fermion $n_i = 4$. The quantum corrections to the potential correspond to the 1-loop vacuum diagrams. They only depend on the effective mass appearing in the propagator, and the results can be extracted from the quadratic potential. The fermion contribution has an overall minus sign as a fermion loop gets an overall sign due to the anti-commuting nature of the fields.

The first term in the brackets in eq. (4.11) is the zero temperature contribution, which sums over the frequencies of all modes – for a free field all the momentum modes are independent harmonic oscillators with zero-point energy $E_{\mathbf{k}} = \frac{1}{2}\omega_{\mathbf{k}}$. This term is

divergent, and the divergence can be absorbed in counter terms of the Lagrangian. This term is the one-loop Coleman-Weinberg contribution to the potential. The 2nd term in the brackets is the finite temperature correction to the potential, which we will denote by $V_T$. The temperature dependent correction is finite, and no temperature dependent counterterms are needed; absorbing counter terms and renormalizing the theory can be done once and for all at $T = 0$.

Note that the effective mass entering $\omega_{\mathbf{k}}$ is background field dependent $m^2 = V''(\phi_0)$, and both terms contribute to the shape of the potential.

### 4.1.2 Thermal corrections to the SM Higgs potential

The temperature corrections come from the one-loop diagrams, with all SM particles running in the loop. These loop diagrams are $\phi$-dependend, as the masses of the particles will depend on the Higgs field value. The EW gauge bosons and the top quark couple most strongly to the Higgs field, and diagrams with these particles in the loop will dominate the thermal corrections to the potential. The potential at one loop order is $V = V_0 + V_{\rm CW} + V_T$, with $V_{\rm CW}$ the zero temperature one-loop correction. The zero temperature contribution is

$$V_0 + V_{\rm CW} = -\frac{1}{2}\mu^2\phi^2 + \frac{1}{4}\lambda\phi^4 + \int \frac{\mathrm{d}^3\mathbf{k}}{(2\pi)^3}\frac{1}{2}\omega_i \left[\sum_{\rm bosons} n_i - \sum_{\rm fermions} n_i\right] \tag{4.12}$$

We can instead work with the RGE improved potential, and work with the classical potential with running couplings. From now on we will ignore the CW contribution, and treat $V_0$ as the zero temperateure RGE improved potential. The thermal potential is eq. (4.11)

$$\begin{aligned} V_T &= \int \frac{\mathrm{d}^3\mathbf{k}}{(2\pi)^3}\left[\sum_{\rm bosons} n_i T\ln(1-\mathrm{e}^{-\beta\omega_i}) - \sum_{\rm fermions} n_i T\ln(1+\mathrm{e}^{-\beta\omega_i})\right] \\ &\overset{T\gg m_i}{=} \sum_i n_i\left(c_i^{(2)}\frac{m_i^2T^2}{24} - c_i^{(3)}\frac{m_i^3T}{12\pi}\right) + \mathcal{O}(m_i^5/T) \end{aligned} \tag{4.13}$$

In the 2nd line we expanded the in large $T^2/m_i^2 \gg 1$. The coefficients are $c_i^{(2)}, c_i^{(3)} = 1$ for bosons, and $c_i^{(2)} = -\frac{1}{2}$ and $c_i^{(3)} = 0$ for fermions. For the SM the largest thermal corrections come from the (Higgs, Goldstone), EW gauge fields, and top quark.

$$\Phi = \{h, \theta, W^\pm, Z, t\}, \quad m^2/\phi^2 = \{3\lambda, \lambda, \frac{1}{4}g^2, \frac{1}{4}(g^2+g'^2), \frac{1}{2}y_t^2\}, \quad n = \{1, 3, 6, 3, 12\} \tag{4.14}$$

In the high temperature expansion $V = V_0 + V_T$ in eqs. (4.12) and (4.13) becomes

$$\begin{aligned} V &= \frac{1}{2}(-\lambda v^2 + aT^2)\phi^2 - \frac{1}{3}bT\phi^3 + \frac{\lambda}{4}\phi^4 \\ &= \frac{1}{2}a(T^2 - \bar{T}^2)\phi^2 - \frac{1}{3}bT\phi^3 + \frac{\lambda}{4}\phi^4 \end{aligned} \tag{4.15}$$

with $\bar{T}^2 = (\lambda/a)v^2$ and

$$a = \frac{1}{2}\lambda + \frac{3}{16}(3g^2 + g'^2) + \frac{1}{4}y_t^2, \qquad b = \frac{1}{16\pi}\left(12(1+\sqrt{3})\lambda + 3g^3 + \frac{3}{2}(g^2 + g'^2)^{3/2}\right) \tag{4.16}$$

The couplings measured at the EW scale are $\{\lambda, g, g'\} \approx \{0.12, 0.38, 0.65\}$.

At high temperature $T^2 > \bar{T}^2 = (\lambda/a)v^2$ the effective temperature dependent mass term is positive, as the positive finite temperature correction exceeds the negative $-\mu^2\phi^2$-term in the Higgs potential. The origin is a minimum of the potential. At high enough temperature this is the only minimum, and the EW symmetry is restored, that is the Higgs field is in the symmetric vacuum phase. As the temperature drops a second minimum appearcs at the critical temperature $T = T_c$, which becomes the true symmetry breaking vacuume of the theory. Whether there is a barrier between the false and true vacuum, and thus whether the PT is 1st or 2nd order, depends on the size of the qubic term, which needs to be large enough for a 1st order PT. Note that only the bosonic fields contribute to this term, as follows from the high temperature expansion eq. (4.13).

The criticical temperature for a 1st order PT is defined as the temperature at which the two minima are degenerate. The potential at the critical temperature can then be written in the following form, with degenerate minima at $\phi = 0$ and $\phi = v_c$

$$V(T_c) = \frac{\lambda}{4}\phi^2(\phi - v_c)^2 = \frac{\lambda}{4}v_c^2\phi^2 - \frac{\lambda}{2}v_c\phi^3 + \frac{\lambda}{4}\phi^4 \tag{4.17}$$

Note that $v_c \neq v$, with $v$ the zero-temperature vev of the higgs field. Comparing **??** and eq. (4.17) gives

$$\frac{1}{2}\lambda v_c = \frac{1}{3}bT_c \quad \& \quad \frac{1}{4}\lambda v_c^2 = \frac{1}{2}a(T_c^2 - \bar{T}^2) \quad \Rightarrow \quad T_c = \frac{\lambda v_c}{\sqrt{a\lambda - \frac{2}{9}b^2}} \tag{4.18}$$

For EW baryogenesis require a strong PT defined as $v_c/T_c \gtrsim 1$. This assures that the washout inside the bubbles of true vacuum is suppressed (and unsuppressed in the surrounding false vacuum phase). This follows from $E_{\rm sph}/T \sim (8\pi/g)(v/T)$, which enters the sphaleron rate $\Gamma \sim \mathrm{e}^{-E_{\rm sph}/T}$, see eqs. (2.30) and (2.33). Hence too avoid too

much washout $v/T$ at bubble nucleation (which we assume is close to the ratio at the critical temperature) should be larger than one. For the SM $v_c/T_c \gtrsim 1$ requires

$$\frac{v_c}{T_c} = \frac{2b}{3\lambda} \approx \frac{3g^3}{16\pi\lambda} \gtrsim 1 \tag{4.19}$$

Thus a strong 1st order PT occurs for a Higgs mass

$$m_H^2 = \frac{1}{2}\lambda v^2 \lesssim \frac{3g^3v^2}{32\pi} = (22\,\mathrm{GeV})^2 \tag{4.20}$$

where we used $v = 246\,\mathrm{GeV}$ and $g = 0.65$. This is much lower than the observed Higgs mass. More careful (lattice) calculations give a larger value for the Higgs mass around 70 GeV to obtain a 1st order PT. Although this is higher, it is still significantly below the observed value.

To get a 1st order PT requires new physics beyond the SM. Additional bosonic fields can enhance the cubic term in the thermal potential, e.g. by adding a singlet (with $Z_2$ symmtry) or Higgs triplet to the SM. In models with singlets (no $Z_2$ symmtry) or additional Higgs doublets, the extra Higgs field can also get a vev in the vacuum, and thus affect the tree-level form of the potential.

### 4.2 Tunneling and bubble nucleation

The time evolution operator of quantum mechanics is $U(t) = \mathrm{e}^{-iHt}$. If the energy, which is the eigenvalue of the Hamiltonian, has an imaginary part $\Gamma \sim \mathrm{Im}(E) \neq 0$, the state will decay. We aim to calculate the decay rate for the false vacuum via bubble nucleation during a first order PT.

Useful reference for phase transitions [9, 14]; the generalization to finite temperature is found in [15].

#### 4.2.1 Tunneling in QM

Start again with QM at zero temperature, and work with Euclidean time. Consider the Euclidean action

$$S_E = \frac{1}{2}\int \mathrm{d}\tau[(\partial_\tau q)^2 + V] \tag{4.21}$$

The potential has (false) vacuum at $q = q_-$ and true vacuum at $q = q_+$ and is normalized such that $V(q_-) = 0$. The equations of motion are

$$\frac{\delta S_E}{\delta q} = -\partial_\tau^2 q + V' = 0 \tag{4.22}$$

These are the equations of motion for a particle moving in a potential $-V$, and $E = \frac{1}{2}(\partial_\tau q)^2 - V$ is a constant of motion. The trivial solution is $q = q_-$, and fluctuations around it correspond in at leading order to the harmonic oscillator:

$$Z = N\mathrm{e}^{-FT} = \int [\mathrm{d}q]\mathrm{e}^{-S_E^{(2)}} = \det[-\partial_\tau^2 + V'']^{-1/2} \sim \mathrm{e}^{-\frac{1}{2}\omega T} \tag{4.23}$$

with $\omega^2 = V''(q_-)$. This gives a shift of the free energy by zero-point fluctuations $F = E_0 = \frac{1}{2}\omega$.

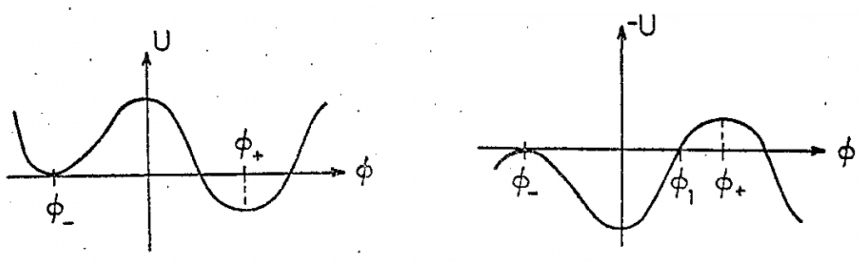


**Figure 5**. Left: Potential $V$ with false and true vacuum. Right: inverse potential $-V$. From [14];

With another local minimum of the potential, there is however another solution to the equations of motions with finite energy. For the energy to be finite $q(\pm T/2) = q_-$ (such that the energy of the field at rest $E = -V$ vanishes), but at intermediate times the field can go to escape point $\sigma$ and back (with $\sigma$ the point for which $V(\sigma) = 0$). This is the bounce solution, which is the solution to the eom with boundary conditions

$$\partial_\tau q|_{\tau_c} = 0, \qquad \lim_{\tau\to\pm\infty} q = q_- \tag{4.24}$$

with $t_c$ the center of the bounce at field value $q(t_c) = \sigma$, and $q = q_-$ asymptotically. Integrate the eom eq. (4.25) to give

$$\partial_\tau(\frac{1}{2}(\partial_\tau q)^2 - V') = 0 \quad \Rightarrow \quad \frac{1}{2}(\partial_\tau q)^2 - V = -V(q_-) = 0 \quad \Rightarrow \quad \tau = \int_q^\sigma \frac{\mathrm{d}q}{\sqrt{2V}} \tag{4.25}$$

The action for the bounce $q_b$ is

$$B \equiv S_E(q_b) = \int \mathrm{d}\tau\, V = \int_0^\sigma \mathrm{d}q\, \sqrt{2V} \tag{4.26}$$

where we used the eom twice to set $\partial_\tau^2 q = V$ and $(\partial_\tau q) = \sqrt{2V}$. There can be many bounces in the time-interval $T$. Summing over them gives

$$\begin{aligned} Z &\sim \mathrm{e}^{-\frac{1}{2}\omega T}\sum_n \int_{-T/2}^{T/2}\mathrm{d}t_1 \int_{-T/2}^{t_1}\mathrm{d}t_2 ... \int_{-T/2}^{t_{n-1}}\mathrm{d}t_n\,(K\mathrm{e}^{-B})^n = \mathrm{e}^{-\frac{1}{2}\omega T}\sum_n \frac{(TK\mathrm{e}^{-B})^n}{n!} \\ &= \mathrm{e}^{-(\frac{1}{2}\omega - K\mathrm{e}^{-B})T} \end{aligned} \tag{4.27}$$

$K$ is the determinant from the gaussian perturbations around the bounce solution. As the bounce is not the minimum of the action but a saddle point, the eigenfunction equation has a negative eigenvalue, and $\mathrm{Im}(K) \neq 0$. Now defining the decay probability per unit time by

$$\Gamma = -2\mathrm{Im}E = \frac{2}{T}\mathrm{Im}\ln Z = 2\mathrm{Im}(K)\mathrm{e}^{-B} = A\mathrm{e}^{-B} = \left(\frac{B}{2\pi}\right)^{1/2}\left|\frac{\det'\left[\partial_\tau^2 + V''(q_b)\right]}{\det\left[\partial_\tau^2 + \omega^2\right]}\right|\mathrm{e}^{-B} \tag{4.28}$$

The action for a single bounce $B$ in eq. (4.26) gives the timescale of decay. Here $\det'$ implies that the zero eigenvalue of the operator $\partial_\tau^2 + V"(q_b)$ is to be omitted. This zero mode corresponds to the time-translational invariance of the bounce solution. We have already included this when integrating over the time translations of the bounce eq. (4.27). The factor $\left(\frac{B}{2\pi}\right)^{1/2}$ comes from the change of variables in the integration of bounce postions to integration of the time of the bounce. The determinant is hard to compute in practice, but the coefficient $A$ can be estimated from dimensional analysis.

### 4.2.2 Tunneling in QFT

Results carry over to QFT. Consider a real scalar with Euclidean action

$$S_E = \int \mathrm{d}^4x \left(\frac{1}{2}(\partial_\tau\phi)^2 + \frac{1}{2}(\nabla\phi)^2 + V\right) \tag{4.29}$$

where the potential has a (false) true vacuum at $(\phi = \phi_-)$ $\phi = \phi_+$, and we set $V(\phi_-) = 0$. The Euclidean Lagrangian is invariant under a four- dimensional Euclidean rotation. The lowest energy bounce solutions is $O(4)$ symmetric. Define $\rho = \sqrt{r^2 + \tau^2}$. The bounce then solves the eom with boundary conditions

$$\Box\phi = \partial_\rho^2\phi + \frac{3}{\rho}\partial_\rho\phi = \partial_\phi V, \qquad \lim_{\rho\to\infty}\phi = \phi_-, \quad \partial_\rho\phi|_{\rho=0} = 0 \tag{4.30}$$

The equation of motion has a mechanical interpretation (with $\rho$ as time) of a particle moving in a potential $-V$, subject to a a damping force (the first derivative term). The particle is released at rest at time zero. If the initial position is chosen properly, this can be done by adjusting the center of the bounce $\phi_b(\rho = 0) = \phi_0$ using a under-shoot/overshoot method, the particle will come to rest at infinite time at $\phi_-$, and the solution has finite energy.

The decay rate per unit volume per unit time is $\frac{\Gamma}{\mathcal{V}} = A\mathrm{e}^{-B}$ with

$$\begin{aligned} B &= S_E(\phi_b) - S_E(\phi_-) = (2\pi^2)\int \mathrm{d}\rho \left[\frac{1}{2}(\partial_\rho\phi_b)^2 + V(\phi_b)) - V(\phi_-)\right], \\ A &= \left(\frac{B}{2\pi}\right)^2 \left|\frac{\det'\left[\partial_\tau^2 + V''(\phi_b)\right]}{\det\left[\partial_\tau^2 + V''(\phi_-)\right]}\right| \end{aligned} \tag{4.31}$$

with $\phi_b$ the bounce solution. $S_E(\phi_-)$ is the action for the trivial solution in the false vacuum, which vanishes with our normalization $V(\phi_-) = 0$. There are now 4 zero modes corresponding to translation of the solution along any of the 4 axes in euclidean space.

At zero temperature the bubbles nucleate because of quantum fluctuations. For $T \neq 0$ thermal fluctuations will also play a role. The dynamics of bubble formation is influenced by temperature.

To include finite temperature one needs to compactify the imaginary time direction $0 < \tau < \beta$. Consider the infinite time axis, where the theory is periodic with period $\beta$. For bubble sizes $R \ll \beta$, i.e. $T < R^{-1}$, the bubble is much smaller than the size of the compactified direction, and the finite temperature effects are small. The solution is a series of the $O(4)$-symmetric bubbles placed at a distance $\beta$ from each other. As $T$ increases the bubbles become placed closer together, until at $T \sim R^{-1}$ they become overlapping in the time direction. For $T \gg R^{-1}$ the solution is a cylinder, whose spatial cross section is the the $O(3)$ symmetric bubble of some new radius. In other words, the bubble solution can be approximated as constant in the time direction, which can be integrated over, and is the solution of the equations of motion in 3 dimensions.

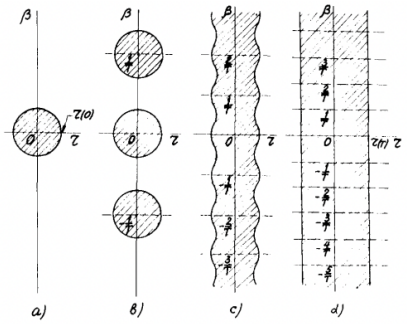


**Figure 6**. Solution of the bounce equations at different values of the temperature. (a) $T = 0$; (b) $T \ll R^{-1}$; (c) $T \sim R^{-1}$; (d) $T \gg R^{-1}$. The dashed regions contain the classical field $\phi \neq 0$. For simplicity we have shown the bubbles for the case when their wall thickness is less than the bubble radius. From [15].

We can then write the euclidean action as

$$B = \int \mathrm{d}\tau \int \mathrm{d}^3\mathbf{r}\, \mathcal{L}_E = \beta S_3, \quad S_3 = \int \mathrm{d}^3\mathbf{r} \left( \frac{1}{2}(\nabla\phi)^2 + V(\phi, T) \right) \tag{4.32}$$

where we again set $V(\phi_-) = 0$. The bubble will now be $O(3)$ symmetric, and the eom become

$$\Box\phi = \partial_\rho^2\phi + \frac{2}{\rho}\partial_\rho\phi = \partial_\phi V, \qquad \lim_{\rho\to\infty} \phi = \phi_-, \quad \partial_\rho\phi|_{\rho=0} = 0 \tag{4.33}$$

with now $\rho = \sqrt{\mathbf{r}^2}$. The different coefficient of the damping term comes from the $\Box\phi$ operator in 3 dimensions. The tunneling rate per unit volume is

$$\frac{\Gamma}{\mathcal{V}} = Ae^{-S_3/T} = \left(\frac{S_3}{2\pi T}\right)^{3/2} \left|\frac{\det'\left[\partial_\tau^2 + V''(\phi_b)\right]}{\det\left[\partial_\tau^2 + V''(\phi_+)\right]}\right| e^{-S_3/T} \tag{4.34}$$

The coefficient $A \sim T^4 \left(\frac{S_3}{2\pi T}\right)^{3/2}$ on dimensional grounds. This gives us an expression for the tunneling rate per unit volume for a given temperature.

### 4.2.3 Thin wall approximation

Consider the limit that the energy-density difference between the true and false vacuum is much smaller than the height of the barrier. We parameterize the potential

$$\epsilon = V(\phi_-) - V(\phi_+), \quad V = V_0 + \epsilon\frac{(\phi - \phi_-)}{(\phi_+ - \phi_-)} \tag{4.35}$$

with $V_0(\phi_+) = V_0(\phi_-) = 0$ the symmetric part of the potential.

The bounce action $S_3$ consists of the surface energy of the bubble proportional to $(\nabla\phi)^2$, which is the transition region in which the field changes from the false vacuum outside the bubble to (close to) the true vacuum inside. The surface term scales as $\propto R^2$ and costs energy. The other term is the volume region inside the bubble $V(\phi_+) - V(\phi_-) = -\epsilon$ for $\rho < R$. This contribution scales as $\propto -\epsilon R^3$ and gains energy. It is energetically favorable for the bubble to expand if the volume term wins. For small $\epsilon$ this happens only for a large radius $R$. When the size of the bubble becomes much larger than the thickness of the wall the bounce solution $\phi(\rho)$ stays close to the escape point at $\rho = 0$ for a long time, until at $\rho \sim R$ it rolls to the asymptotic false vacuum solution at $\phi_-(\rho \to \infty)$. The thin wall approximation consists of dropping the damping term in the eom. At small $\rho$ it is negligible because the field is approximately frozen, whereas when it starts to roll at large radius $\rho \sim R$ the damping term is $1/R$ suppressed.

Dropping the friction term and the $\epsilon$-correction to the potential in the eom eq. (4.33) gives $\phi'' = \partial_\phi V_0$. We have already solved this in the QM example eq. (4.25). Copying that solution gives

$$\rho - \bar{\rho} = \int_{\frac{1}{2}(\phi_- + \phi_+)}^{\phi} \frac{d\phi}{\sqrt{2V_0}} \tag{4.36}$$

with $\bar{\rho}$ the integration constant defined as the coordinate when $\phi(\rho)$ is the average of the two minima.

If $\bar{\rho}$ is large, the bounce looks like a ball of true vacuum, $\phi = \phi_+$, embedded in a sea of false vacuum, $\phi = \phi_-$, with a transition region ("the wall") separating the two. The wall is small in thickness compared to the radius of the ball $\bar{\rho}$. We can divide

the solution in three regions: $\phi = \phi_-$ in the outside region $\rho > \bar{\rho}$, $\phi = \phi_+$ in the inside region $\rho < \bar{\rho}$, and the wall region $\rho \sim \bar{\rho}$ wherec the transition takes place. The euclidean action is

$$\begin{aligned}(S_3)_{\text{outside}} &= 0, \\ (S_3)_{\text{inside}} &= -\frac{4}{3}\pi\bar{\rho}^3\epsilon, \\ (S_3)_{\text{wall}} &\approx 4\pi\bar{\rho}^2 \int \mathrm{d}\rho\,(2V_0) = 4\pi\bar{\rho}^2 \int_{\phi_+}^{\phi_-} \mathrm{d}\phi\,\sqrt{2V_0} \equiv 4\pi\bar{\rho}^3 S_1\end{aligned} \tag{4.37}$$

where we assumed the wall thickness much smaller than $\bar{\rho}$. $S_1$ is the action for the 1-dim theory, which gives the surface tension of the bubble. To find the radius $R$, minimize the action with respect to $\bar{\rho}$

$$\partial_{\bar{\rho}} S_3\Big|_{\bar{\rho}=R} = \partial_{\bar{\rho}}\left(-\frac{4}{3}\pi\bar{\rho}^3\epsilon + 4\pi\bar{\rho}^2 S_1\right)\Big|_{\bar{\rho}=R} \quad \Rightarrow \quad R = \frac{2S_1}{\epsilon} \tag{4.38}$$

which gives

$$S_3 = \frac{16\pi S_1^3}{3\epsilon^2} \tag{4.39}$$

as the final result.

### 4.2.4 Fate of the false vacuum

Consider first the $T = 0$ case. The classical field makes a quantum jump (say at $t = 0$) to the state defined by

$$\phi(t = 0, \mathbf{x}) = \phi(\tau, \mathbf{x}) \tag{4.40}$$

This implies that the same function, $\phi(\rho)$, that gives the shape of the bounce in four dimensional Euclidean space also gives the shape of the bubble at the moment of its materialization in three-space. At finite $t$ we can analytically continue back to minkowski space to find

$$\phi(t, \mathbf{x}) = \phi(\rho = \sqrt{|\mathbf{x}|^2 - t^2}) \tag{4.41}$$

The bubble will expand (or collapse), with velocity that soon after its existence will reach the speed of light. The energy is the sum of the negative volume energy term and a positive surface term. For the thin wall solution

$$E = -\frac{4\pi}{3}\epsilon R^3 + 4\pi S_1 R^2 = \frac{4\pi}{3}\rho^2(R_0 - R)\epsilon \tag{4.42}$$

with $R_0$ the radius of the thin wall bubble at creation. The energy vanishes at bubble creation, dictated by energy conservation, as the energy vanished before the bubble was

created. The bubble will expand if the volume term wins and $\partial_R E \geq 0$. The critical bubble where this equation is saturated has $R_c = 2S_1/\epsilon$. Since $R_0 > R_c$ the thin wall bubble will expand.

For the thin wall solution the bubble has a thin wall at $R = R_0$. As the bubble expands, this wall traces out the hyperboloid $|\mathbf{x}|^2 - t^2 = R_0^2$, and the ball expansion soon reaches the speed of light.

At finite temperature the ball will not expand in vacuum but in a thermal plasma. Plasma particles will scatter off and enter the bubble, and as they are massless outside and massive inside, this will take away energy, slowing the bubble down. To calculate the bubble expansion velocity is a very active area of research, as this parameter enters the predictions for baryogenesis and the gravitational wave signal.

**Nucleation temperature.** The phase transtion occurs if the bubbles expand and coalesce, and the whole of space thus transitions to the true vacuum state. For this to happen, at least one bubble per Hubble volume per Hubble time needs to be nucleated. In other words, when $\Gamma \sim H$ – where we used that $\mathcal{V} \sim H^{-3}$ is equal to the Hubble volume – the phase transtion takes place. The temperature at which this happens is called the nucleation temperature $T_N$, which is lower than the critical temperature. For strong phase transtions, happening for potentials with a large barrier, the phase transition can be delayed with nucleation temperature much smaller than the critical temperature; if the barrier is really large, the universe may be stuck in the false vacuum (on timescales of the age of the universe) and the phase transition never takes place. In the opposite limit, for shallow barriers, one expects $T_N \sim T_c$ to be close.

Using that $H^2 \sim T^4/M_{\rm P}^2$ during radiation domination, one can estimate the nucleation temperature via

$$\frac{S_3}{T} \sim \ln(H^4/T^4) \sim \ln(M_{\rm P}^4/T^4) \tag{4.43}$$

For the EW scale $T \sim 10^2\,\text{GeV}$ this gives $S_3/T_N \sim 150$.

### 4.3 Sketch of EW baryogenesis calculation

The calculation of the final asymmetry is complicated, because of finite temperature effects (and e.g. the IR contributions of soft photons), non-equilibrium dynamics, and non-perturbative dynamics. Calculations are usually done in a EFT-like approach, where proccesses on different timescales are separated. Let's assume the bubble wall background is changing slowly on the time-scales of the CP-violating plasma interactions, and can be treated as adiabatically changing. The sphaleron transitions are also relatively slow, and the process can be considered as a two step process: first a chiral

asymmetry is created, and then at a later time this is transferred into a baryon asymmetry. The calculational approach will then be to determine the phase space densities of the plasma particles interacting with the slowly changing bubble wall background.

Consider the distribution function $f(\mathbf{x}, \mathbf{p}, t)$, which is a function of position, proper momentum and time. It describes the density of particles at time $t$, at the point $\mathbf{x}$ and with momentum $\mathbf{p}$. (Quantum mechanically no particle can be localized in phase space at a point $(\mathbf{x}, \mathbf{p})$, and one should integrate over a (small) phase space volume to get the propability to find a particle in that volume.) Integrating the distribution function over momenta gives the particle number density:

$$n(\mathbf{x}, t) = g_s \int \frac{\mathrm{d}^3\mathbf{p}}{(2\pi)^3} f(\mathbf{x}, \mathbf{p}, t) \tag{4.44}$$

with $g_s$ the degeneracy of the species, e.g. the number of spin or polarization states. In a constant background and in thermal equilibrium the phase-space density is space-time independent, and it is the familiar Bose-Einstein and Fermi-Dirac distribution for bosons and fermions $f = (\mathrm{e}^{\sqrt{k^2+m^2}/T} \pm 1)^{-1}$. For a system close to thermal equilibrium one can perturb around the equilibrium distributions, and try to solve for the perturbations. The time evoltion of the phase space densities is given (at the semi-classical level) by the Boltzmann equations:

$$\frac{\mathrm{d}f}{\mathrm{d}t} = C[f] \tag{4.45}$$

with $C[f]$ the collision term which describes the interaction among the particles. Out of equilibrium both positon and momentum are generically a function of time, and the total time derivative can be written as

$$\frac{\mathrm{d}f}{\mathrm{d}t} = \frac{\partial f}{\partial t} + \frac{\mathrm{d}\mathbf{x}}{\mathrm{d}t} \cdot \nabla_{\mathbf{x}} f + \frac{\mathrm{d}\mathbf{p}}{\mathrm{d}t} \cdot \nabla_{\mathbf{p}} f = \frac{\partial f}{\partial t} + \mathbf{v} \cdot \nabla_{\mathbf{x}} f + \mathbf{F} \cdot \nabla_{\mathbf{p}} f \tag{4.46}$$

where $\mathbf{v}$ is the particle velocity and $\mathbf{F}$ is the force acting on the particle.

The CP violating yukawa interaction eq. (4.1) gives a complex mass term

$$m(\mathbf{x}, t) = \frac{y_t}{\sqrt{2}} v_b (1 + c\frac{v_b^2}{2\Lambda^2}) = |m| \mathrm{e}^{i\theta} \tag{4.47}$$

with $v_b$ the bubble background: $v_b = 0$ outside the bubble and $v_b = v_N$ at nucleation temperature inside the bubble, and the change in the bubble wall is given by the bounce solution. Taking for simplicity $c = ic_I$ imaginary, then $|m| = \frac{y_t}{\sqrt{2}} v_b$ and $\theta = \frac{c_I}{y_t} \frac{v_b^2}{2\Lambda^2}$ up to higher order corrections in $\Lambda^{-2}$. This generates a force when a particle tries to enter the bubble wall, as momentum is needed to generate the mass inside and thus $\dot{p} \neq 0$.

For a complex mass this source is different for particles and antiparticles. To calculate the force one needs to find the dispersion relation $E(p)$ in the bubble wall background, which allows to extract the force $\dot{\mathbf{p}}$.

Start with the Dirac equation for the top quark, which can be written as

$$(i\partial\!\!\!/ - mP_L - m^* P_R)\psi = 0 \tag{4.48}$$

with $P_{L,R} = \frac{1}{2}(1 \mp \gamma_5)$. Go the frame in which the bubble wall is at rest. Now decompose the spinor into its chiral compoments as

$$\psi = \begin{pmatrix} q_L \\ q_R \end{pmatrix} = \mathrm{e}^{-i\omega t} \begin{pmatrix} L_s \\ R_s \end{pmatrix} \otimes \chi_s \tag{4.49}$$

These are positive energy solutions, appropiate for particles. We will use the chiral basis for the gamma matrices

$$\gamma^\mu = \begin{pmatrix} 0 & \sigma^\mu \\ \bar{\sigma}^\mu & 0 \end{pmatrix}, \quad \text{with } \sigma^\mu = (1, \sigma^i) \ \ \& \ \ \bar{\sigma}^\mu = (1, -\sigma^i). \tag{4.50}$$

$\chi_s$ is a two component spinor state with $\sigma^3 \chi = s\chi$, and $s$ labeling the spin along the direction of motion, which we take the $z$-direction. The dirac equation becomes

$$(\omega - is\partial_z) L_s = m R_s, \quad (\omega + is\partial_z) R_s = m^* L_s \tag{4.51}$$

These can be written as uncoupled 2nd order equations

$$\left[ (\omega + is\partial_z) \frac{1}{m} (\omega - is\partial_z) - m^* \right] L_s = 0, \quad \left[ (\omega - is\partial_z) \frac{1}{m^*} (\omega + is\partial_z) - m \right] R_s = 0 \tag{4.52}$$

After Fourier transform $L_s(z) = \int \frac{\mathrm{d}^3 k}{(2\pi)^3} \mathrm{e}^{ikz} L_s(k)$ this gives for aconstant $m$ the solution $\omega^2 - k^2 - |m|^2 = 0$, which is the usual dispersion relation for a free particle. In a spacetime-dependent background $p = p(z)$, giving rise to a non-zero force $\dot{p}$ in the dispersion relation; if $m \neq m^*$ the force can be different for the left- and right-handed modes. To solve the equations, assume the bubble wall background is slowly changing, and use the WKB Ansatz

$$L_s = \omega(z) \mathrm{e}^{i \int^z p(z') \mathrm{d}z'} \tag{4.53}$$

Substitute in the Dirac equation for $L_s$, and solve iteratively in a derivative expansion. The solution is

$$p = p_0 + \frac{s\omega + p_0}{2p_0} \theta' + \mathcal{O}(\partial_z^2), \quad p_0 = \mathrm{sign}(p) \sqrt{\omega^2 - |m|^2} \quad \Rightarrow \quad \omega = \sqrt{(p + \theta'/2)^2 + |m|^2} - \frac{1}{2} s\theta' \tag{4.54}$$

For anti-particles can repeat the caculation for negative energy modes. Results is to set $m \to -m^*$, which changes $\theta' \to -\theta'$. Finally, to compute the force entering the Boltzman equation we use the Hamilton equation

$$\dot{p} = -\left(\frac{\partial\omega}{\partial_z}\right)_p = -\frac{(m^2)^2}{2\omega} + ss_c\frac{(m^2\theta')'}{2\omega^2} \tag{4.55}$$

with $s_c = \pm 1$ for particles and antiparticles. The first is a CP conserving force term, the same for particles and antiparticles. As it is larger, it is the dominant friction term as the bubble expands in the plasma, and important to find the expansion velocity of the bubble. The 2nd term is the CP-violating force term, that may generate a chiral asymmetry between left-handed particles and antiparticles. The Boltzman equation is a partial differential equation. It can be solved approximately taking moments, to find the net chiral asymmetry.

The finaly baryon asymmetry is then

$$\frac{\mathrm{d}n_B}{\mathrm{d}t} \sim N_f\Gamma_{\rm sph}\mu_{t_L} - c\Gamma_{\rm sph}\frac{n_b}{T^2} \tag{4.56}$$

The first term converts an overdensity of left-handed (anti)-particles into a baryon asymmetry, note that the chemical potential $\mu_{q_L}$ for the left-handed tops is proportional $n_{t_L} - n_{\bar{t}_L}$. The 2nd term is the washout term, the more baryons are created, the more important it becomes. The sphaleron rate $\Gamma_{\rm sph}(x)$ is only important outside the bubbles, where baryons can be created, and it becomes small inside the bubble where the transitions are shut off. In the bubble wall rest-frame, the frame that the bubble is at rest, one thus should only integrate the above equation in the $z$-region outside the bubble.

### 4.4 Constraints from electric dipole moment measurements

In non-relativistic electrodynamics the interaction of a fermion with spin $\mathbf{S} = \frac{1}{2}\boldsymbol{\sigma}$ with an electric and magnetic field is described by the Hamiltonian

$$H = -\mu(\mathbf{S}\cdot\mathbf{B}) - d(\mathbf{S}\cdot\mathbf{E}) \tag{4.57}$$

with $\mu$ and $d$ the magnetic and electric dipole moment respectively. Turning on a magnetic (electric) field puts a torque on the system leading to spin prececssion with angular velocity $\omega = 2\mu|\mathbf{B}|\sin\theta$ $(\omega = 2d|\mathbf{E}|\sin\theta)$.

Under a time-reversal $T:\ t \to -t$ and parity $P:\ \mathbf{x} \to -\mathbf{x}$

$$\begin{array}{llll} T: & \mathbf{S}\to -\mathbf{S}, & \mathbf{B}\to -\mathbf{B}, & \mathbf{E}\to \mathbf{E}, \\ P: & \mathbf{S}\to \mathbf{S}, & \mathbf{B}\to \mathbf{B}, & \mathbf{E}\to -\mathbf{E}, \end{array} \tag{4.58}$$

The transformations of $E, B$ can be deduced from the Lorentz force $\mathbf{F} = m\mathbf{a} = q(\mathbf{E} + \mathbf{v} \times \mathbf{B})$, under $T$: $\mathbf{a} \to \mathbf{a}$ and $\mathbf{v} \to -\mathbf{v}$, while under $P$: $\mathbf{a} \to -\mathbf{a}$ and $\mathbf{v} \to -\mathbf{v}$. Spin behaves just as angular momentum $\mathbf{L} = \mathbf{r} \times \mathbf{p}$. Magnetic dipole moments (MDMs) are invariant under $T$ and $P$, but electric dipole moments (EDMs) violate both $T$ and $P$. The CPT theorem tells that $T$ violation is equivalent to $CP$ violatioin. Hence, measurement of an EDM is a probe of CP violation.

The Dirac Lagrangian for a fermion

$$\mathcal{L} = \bar{\psi} i \not{D} \bar{\psi} - m \bar{\psi} \psi \tag{4.59}$$

with covariant deriavite $D_\mu = \partial_\mu + ieA_\mu$, gives in the non-relativistic limit a MDM with $\mu = eg/(2m)$ and $g = 2$, but no EDM $d = 0$. This can be seen by calculating the tree-level diagram in fig. 7. The absence of an EDM is expected as QED does not violate CP. The MDMs and EDMs get loop level contributions

$$\delta\mathcal{L} = -\frac{1}{2} \bar{\psi} \sigma^{\mu\nu} (\frac{ea}{m} + i\gamma^5 d) \psi F_{\mu\nu} \tag{4.60}$$

with $a = (g-2)/2$ the anomalous magnetic moment. In the SM there is CP violation in the CKM matrix (and in the $\theta$-term, which we ignore). Consider the electric dipole moment of the electron, which has been measured very precisely, and generically gives the stronges bounds on CP violation. At one loop there are only CP conserving diagrams in the SM, see fig. 7, contributing to $a$ but not $d$. Only at 4 loops is the electron EDM first generated from CKM-interactions. In SM the electron magnetic and electric dipole moments are

$$\mu_e \simeq 100\, e\,\text{fm}, \qquad d_e \simeq 10^{-2e}\, e\,\text{fm}, \tag{4.61}$$

The CKM EDM is really small.

Currently the strongest bound on the electron EDM come from the [**?** ] experiment, which give the constraint $d_e \lesssim 10^{-29}\, e\,\text{cm} = 10^{-16}\, e\,\text{fm}$. The sensitivy is way off to measure the CKM EDM. However, if new CP violating physics exist this can give a dominant contribution to the EDM, and the ACME results are actually a quite powerfull constraint. On dimensional grounds a tree-level contribution to the electron EDM by new physics at a scale $\Lambda$ will be of the order

$$d_e \sim \frac{m_e}{\Lambda^2} e \sim 4 \times 10^{-24} \left(\frac{\text{TeV}}{\Lambda}\right)^2 e\,\text{cm} \leq 4 \times 10^{-30}\, e\,\text{cm} \tag{4.62}$$

which gives the constraint $\Lambda \gtrsim 10^3\,\text{TeV}$. If the EDM is generated at $n$-loop level, we expect $n$ loop factors $(4\pi)^2$ (and possibly further suppression by small couplings), reducing the bound on $\Lambda$. Still, bounds can be much stronger than currenly probed in the LHC.

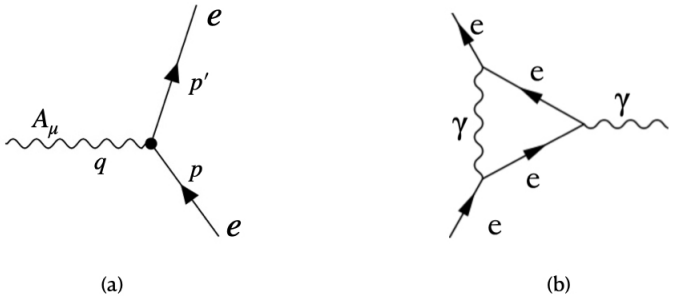


**Figure 7**. Tree level (a) and one-loop (b) contribution to the magnetic dipole moment of the electron within QED.

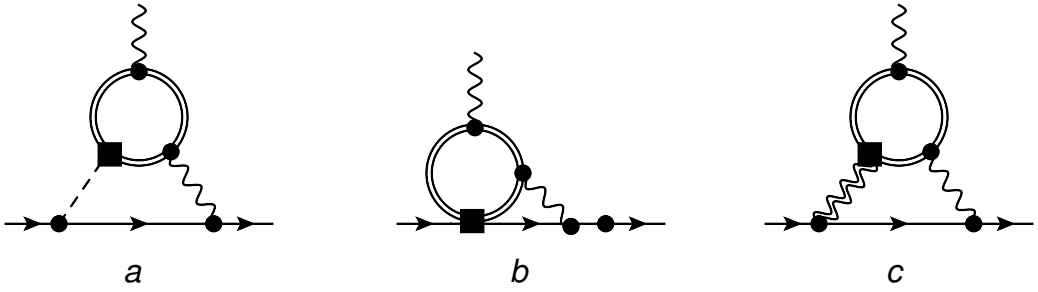


**Figure 8**. Two-loop diagrams contributing to the electron EDM. Single (double) lines denote the electrons (top quarks), dashed lines the Higgs boson, and wavy single (doubles) lines the photons (Z-bosons). Circles denote SM vertices, while squared denotes CPV dimension-six vertices. Only one topology for each diagram is shown.

If we consider the CP violating correction to the top yukawa coupling that we looked at before eq. (4.1), this generates an EDM at two-loop level, see fig. 8

$$\frac{d_e}{e} = -\frac{8\alpha_{\rm em}}{(4\pi)^3} m_e N_c Q_t^2 g(x_t) \frac{\mathrm{Im}(c)}{\Lambda^2}, \quad g(x_t) = \frac{x_t}{2}\int_0^1 \mathrm{d}x \frac{1}{x(1-x)-x_t} \ln\left(\frac{x(1-x)}{x_t}\right) \tag{4.63}$$

with $x_t = m_t^2/m_h^2$, and numerically the two-loop function is $g(x_t) \approx 1.4$. For $\mathrm{Im}(c) = 1$ this gives the very strong bound $\Lambda \geq 7.1\,\mathrm{TeV}$ on the cutoff scale.

The EDM bound rules out the simplest scenarios for EW baryogenesis, as the CP violation is too small to obtain the observed baryon asymmetry. Solutions are a fine-tuning in the CP violating couplings such that there is a partial cancellation in diagrams contributing to the EDM, thus weakening the bound on the cutoff scale. CP

violating couplings to other scalar fields (e.g. the singlet in the doublet-singlet model) are unconstrained by EDM measurements. Yet, another avenue is to consider different mechanism for EW baryogenesis. E.g. one could consider resonance effects in EW baryogensis with multiple fermion flavors. Or a set-up where the plasma particles are (temporarily) trapped in the pockets of false vacuum phase (as it cost energy to enter the bubble), increasing their local density.

### 4.5 Constraints from gravitational waves

The Einstein's equations

$$R_{\mu\nu} - \frac{1}{2} R g_{\mu\nu} = 8\pi G_N T_{\mu\nu} \tag{4.64}$$

describe how spacetime curves in the presence of matter, and how matter moves in a curved spacetime. The curvature tensor and scalar are constructed from the metric, which measures distances

$$\mathrm{d}s^2 = g_{\mu\nu} \mathrm{d}x^\mu \mathrm{d}x^\nu \tag{4.65}$$

with summation over repeated indices implied. In flat spacetime the metric is $g_{\mu\nu} = \eta_{\mu\nu} = \mathrm{diag}(1, -1, -1, -1)$ of Minkowski spacetime, while e.g. in an isotropic and homogeneous expanding universe the metric is the Friedman-Robertson-Walker eq. (A.1). The coupling between the curvature on the lhs and the energy-momentum on the rhs of the Einstein equations is suppressed by $8\pi G_N = 1/M_{\rm P}^2$. Around most astrophysical objects such as our sun the gravitational field is weak, with curavure radius $R^{-2}$ much smaller than the planck length (the exception of strong gravituational fields are black holes, and near the big bang). We can then perturb the metric around the FRW background and linearize the (non-linear) Einstein equations. Any causal mechanism can only produce gravitational waves on subhorizon scales, where curvature effects are small, and for simplicity we neglect the expansion of the universe for now.

Expanding the metric $g_{\mu\nu} = \eta_{\mu\nu} + \tilde{h}_{\mu\nu}$ with $|\tilde{h}_{\mu\nu}| \ll 1$, substituting in Einstein's equations and using Lorentz gauge $\partial^\nu \tilde{h}_{\mu\nu} = 0$ gives

$$\Box h_{\mu\nu} = -16\pi G_N T_{\mu\nu} \tag{4.66}$$

with $h_{\mu\nu} = \tilde{h}_{\mu\nu} - \frac{1}{2}\eta_{\mu\nu}\tilde{h}$. The metric is a symmetric $4 \times 4$ real tensor, which has 10 dof. The gauge fixing removes 4 dof. The Einstein equation ouside the source ($T_{\mu\nu}$) gives 4 constraint equation, which we can use to go to transverse-traceless gauge

$$h_{\mu 0} = 0, \quad h^j_j = 0, \quad h^j_{ij,} = 0 \tag{4.67}$$

The first condtion set all temporal components to zero, the 2nd are the traceless and transverse conditions. In this gauge $\tilde{h}_{\mu\nu} = h_{\mu\nu}$. The existence of the 4 constraint

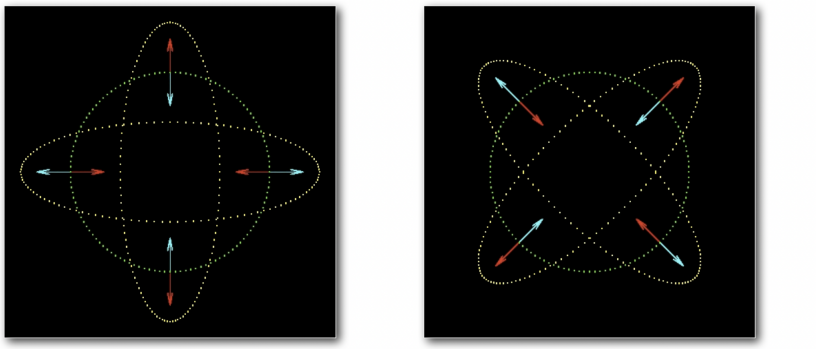


**Figure 9**. Polarizations for a gravitational wave travelling out of the plane

equations can be understood because the Lorentz gauge does not fix gauge invariance fully. There are gauge transformations $x^{\mu'} \to x^\mu + \xi^\mu$ that leave the lorentz gauge condition invariant, $\tilde{h}'_{\mu\nu} = \tilde{h}_{\mu\nu} - (\xi_{\mu,\nu} + \xi_{\nu,\mu})$ with $\Box\xi^\mu = 0$. This additional freedom allows to go to transverse-traceless gauge. The end result is that there are two physical dof, corresponding to the two polarizations.[8]

In a cosmological context, the gravitational wave (GW) can be described by a tensor perturbation of the FRW metric eq. (A.1)

$$\mathrm{d}s^2 = \mathrm{d}t^2 - a^2(\delta_{ij} + h_{ij})\mathrm{d}x^i\mathrm{d}x^j \tag{4.68}$$

which is transverse and traceless $\partial_i h_{ij} = h_{ii} = 0$. $h_{ij}$ is symmetric and has 6 dof, the gauge constraints fix four, which leaves two dof corresponding to the polarizations.

In vacuum $T_{\mu\nu} = 0$ eq. (4.66) is a wave equation. If we consider a wave travelling along the $z$-direction the solution is (in TT gauge)

$$h_{ij}(t,z) = \begin{pmatrix} h_+ & h_\times \\ h_\times & -h_+ \end{pmatrix} \cos(\omega(t-z)) \tag{4.69}$$

with $h_+, h_\times$ the amplitudes of the two polarizations. The gravitational wave travels with the speed of light.

[8] This can be compared with electromagnetism where the vector field $A^\mu$ has 4 dof, there is one gauge fixing condition e.g. $\partial^\mu A_\mu = 0$, which only partially fixes the gauge as transformations $A^{\mu'} = A^\mu + \partial^\mu\epsilon$ leave the gauge condition invariant for $\Box\epsilon = 0$. This additional freedom allows to eliminate another dof, or equivalently, the $A_0$ equations is non-dynamical and provides a constraint on the system. There are then two phyiscal dof (the two polarizations).

If we put the source term back in we can solve the eq of motion by Green's functions methods $\Box_x G(x,x') = \delta^4(x-x')$. We are interested in the retarded Green's functions, such that the solution only depends on past sources and is causal – this is analogous to what is used in electrodynamics. Using that $\nabla^2(1/|\mathbf{x}-\mathbf{x}'|) = -4\pi\delta^3(\mathbf{x}-\mathbf{x}')$ gives

$$\begin{aligned} h_{ij}^{TT} &= \frac{16\pi G_N}{4\pi}\int \mathrm{d}t' \int \mathrm{d}^3x' \frac{T_{ij}^{TT}(x',t')}{|\mathbf{x}-\mathbf{x}'|}\delta(t'+|\mathbf{x}-\mathbf{x}'|-t) \\ &= \frac{16\pi G_N}{4\pi}\int \mathrm{d}^3x' \frac{T_{ij}^{TT}(x',t-|\mathbf{x}-\mathbf{x}'|)}{|\mathbf{x}-\mathbf{x}'|} \end{aligned} \tag{4.70}$$

with $T^{TT}$ the transverse traceless part of the energy-momentum tensor. For an observer far from the source $kr \gg 1$ we can make the approximation $|\mathbf{x}-\mathbf{x}'| = r - \hat{\mathbf{n}}\cdot\mathbf{x}'$ (with $r = |\mathbf{x}|$). We further assume the source is non-relativistic, such that we can neglect internal motions of the source. We can then do a multipole moment expansion in $(\hat{\mathbf{n}}\cdot\mathbf{x}')$. Keeping only the leading order term, this gives

$$h_{ij}^{TT} \approx \frac{16\pi G_N}{4\pi r}\int \mathrm{d}^3x\, T_{ij}^{TT}(x,t-r) \tag{4.71}$$

Finally, using energy momentum conservation $\partial_\mu T^{\mu\nu} = 0$ one can show that $\int \mathrm{d}^3x\, T^{ij} = \frac{1}{2}\frac{\partial^2}{\partial t^2}\int \mathrm{d}^3x\, T^{00}x^i x^j$ and

$$h_{ij}^{TT} \approx \frac{16\pi G_N}{8\pi r}\frac{\partial^2}{\partial t^2}\int \mathrm{d}^3x\, T_{00}(x,t-r)(x^i x^j - \frac{1}{3}\delta^{ij}r^2) = \frac{16\pi G_N}{8\pi r}\ddot{Q}_{ij} \tag{4.72}$$

with $Q^{ij} = \int \mathrm{d}^2x\, T^{00}(x^i x^j - \frac{1}{3}\delta^{ij}r^2)$ the quadrupole moment, and (for weak fields) $T^{00} = \rho$ the energy density. The delta function term is added to pick the transverse traceless part of the energy momentum tensor.

If a gravitational wave passes two test particles at rest located at $\mathbf{x} = (0,0,0)$ and $\mathbf{x} = (\epsilon,0,0)$, the proper distance between them changes as

$$l = \int \sqrt{\mathrm{d}s^2} = \int_0^\epsilon \sqrt{|g_{xx}|}\mathrm{d}x \simeq (1+\frac{1}{2}h_{xx}(x=0))\epsilon \tag{4.73}$$

The gravitational wave is curving the spacetime, which we can detect by the geodesic deviation it introduces.

Gravitational waves are generated by accelerated mass distributions with a non-zero quadrupole moment. Spherical system will not produce a gravitational wave signal, as the quadrupole is zero, but any deviation from spherical symmetry can. Also the system must be accelerating, and a system in stationary motion does not radiate. As the coupling is $8\pi G_N = 1/M_{\mathrm{P}}^2$ suppressed, these sources must be energetic to obtain observable waves, especially if the sources are far away.

### 4.5.1 GW from 1st order PT

The energy density in gravitational waves is

$$\rho_{\rm gw} = \frac{\langle \dot{h}_{ij}\dot{h}_{ij}\rangle}{4\pi} = \int \frac{{\rm d}f}{f}\frac{{\rm d}\rho_{\rm gw}}{{\rm d}\log f} \tag{4.74}$$

with $f$ the frequency, and from now on we set $8\pi G_N = 1$. The superposition of GW produced by a large number of unresolved sources in the early universe form a stochastic background, assumed to be statistically isotropic, stationary and nearly Gaussian. Its main properties are then described by its power spectrum. The quantity that is usually considered to characterize cosmological backgrounds is the spectrum of energy density per logarithmic frequency interval divided by the critical density $\rho_{c,0}$ today

$$h^2\Omega_{\rm gw}(f) = \left(\frac{h^2}{\rho_c}\frac{{\rm d}\rho_{\rm gw}}{{\rm d}\log f}\right)_0 \tag{4.75}$$

with $\rho_{c,0} = 3H_0^2$ and $H_0 = 100h\,{\rm km/s/Mpc.}$, and $h$ parameterizing the uncertainty in todays Hubble constant.

Let's start with an estimate of the typical frequency and signal for a first order PT, which can be sourced by colliding bubbles and plasma waves that are accelerated by the bubbles.

The time of the PT is the nucleation temperature $T_* \approx T_n$. The inverse time duration of the transition is parameterized by $\delta t_*^{-1} = \beta$. For subhorizon causal mechanisms $\beta/H_* > 1$; in the case of a PT this is the requirement that the PT ends and bubbles coalesce. $\beta$ can be defined from the bubble nucleation rate eq. (4.34) via

$$\beta = -\frac{{\rm d}(S_3/T)}{{\rm d}t}\Big|_* \simeq \frac{\dot{\Gamma}}{\Gamma} \quad \Rightarrow \quad \frac{\beta}{H_*} = T\frac{{\rm d}(S_3/T)}{{\rm d}T}\Big|_* \tag{4.76}$$

The bubble wall radius can be estimated $R \sim v_w/\beta$ with $v_w$ the expansion velocity of the bubble. The characteristic wave number of the gravitational wave is then of the order $k_* \sim 1/R = \beta/v_w$, corresponding to a frequency $f_* = k_*/(2\pi)$. The energy density can be estimated from the eom eq. (4.66). A time-derivate gives a $\beta$-factor, and schematically the eom becomes $\beta^2 h^2 \sim 2T$, which suggests $\dot{h} \sim 2T/\beta$. Then $\rho_{\rm gw} \sim \dot{h}^2/(4\pi) \sim T^2/\beta^2$. Setting $T \sim \rho_s$ equal to the energy in the source (released in the PT transition) and dividing by the total (critical) energy density at time of emission this gives $\rho_{\rm gw}/\rho_c \sim (H_*/\beta)^2(\rho_s/\rho_c)_*^2$.

To relate the frequency and energy denisity at emission to what is observed today one has to take the expansion of the universe into account. The energy density in gravity waves decreases as $a^{-4}$ and the frequency of the gravity waves redshifts as $a^{-1}$, with $a$

the scale factor. If the universe has expanded adiabatically since the phase transition, the entropy per comoving volume $S = a^3 g_*(T) T^3$ remains constant eq. (A.21), and the ratio of the scale factor at the transition to the scale factor today is

$$\frac{a_*}{a_0} = 8 \times 10^{-17} \left(\frac{100}{g_*}\right)^{1/3} \left(\frac{1\,\text{TeV}}{T_*}\right) \tag{4.77}$$

The frequency today is then

$$f_0 = f_* \frac{a_*}{a_0} \simeq 10^{-2} \frac{1}{v_w} \frac{\beta}{H_*} \frac{T_*}{100\,\text{GeV}} \left(\frac{g_*}{100}\right)^{1/6} \text{mHz} \tag{4.78}$$

where we used that $H_*^2 = \rho_{\text{rad}}/3 = \pi^2 g_* T_*^4/90$ to write it in terms of the ratio $\beta/H_* > 1$. This falls in the frequency range for LISA which has largest sensitivity in the mHz range.

The GW are produced in the radiation dominated era, but at later times the universe became matter and cosmological constant dominated. Radiation red shifts as

$$\frac{\rho_{\text{rad}}(T_0)}{\rho_{\text{rad}}(T_*)} = \frac{g_*(T_0) T_0^4}{g_*(T_*) T_*^4} = \left(\frac{g_*(T_*)}{g_*(T_0)}\right)^{1/3} \frac{a_*^4}{a_0^4} \quad \Rightarrow \quad \frac{\Omega_{\text{gw}}}{\Omega_{\text{rad}}} = \left(\frac{\rho_{\text{gw}}}{\rho_{\text{rad}}}\right)_0 = \left(\frac{g_*(T_*)}{g_*(T_0)}\right)^{1/3} \left(\frac{\rho_{\text{gw}}}{\rho_{\text{rad}}}\right)_* \tag{4.79}$$

The only difference between the plasma and GW energy densities, is that the former gets slightly heated each time a dof freezes out; this effect is incorporated in the time-dependence of the number of relativistic dof $g_*$. As the GW are produced during radiation domination $\rho_{\text{rad}}(T_*) = \rho_c(T_*)$ at the time of emission, and we can thus write

$$\Omega_{\text{gw}} = \Omega_{\text{rad}} \left(\frac{g_*(T_*)}{g_*(T_0)}\right)^{1/3} \Omega_{\text{rad}} \left(\frac{\rho_{\text{gw}}}{\rho_c}\right)_* \sim \Omega_{\text{rad}} \left(\frac{g_*(T_*)}{g_*(T_0)}\right)^{1/3} \left(\frac{H_*}{\beta}\right)^2 \left(\frac{\rho_s}{\rho_c}\right)_*^2 \tag{4.80}$$

The energy density in GWs is maximised for small $\beta$ (but $\beta$ exceeds unity), and for larger energy release during the PT. Since $h^2 \Omega_{\text{rad}} \simeq 4 \times 10^{-5}$ and within the SM $\left(\frac{g_*(T_*)}{g_*(T_0)}\right)^{1/3} = \mathcal{O}(1)$ a GW signal above the LISA sensitivity of $h^2 \Omega_{\text{gw}} \sim 10^{-12}$ at mHz requires $(H_*/\beta)(\rho_s/\rho_{\text{tot}})_* \gtrsim 10^{-4}$. Detectible signals only arise from slow and very energetic processes.

For a 1st order PT there are three contribution to the source.

- Collisions of bubble walls and (where relevant) shocks in the plasma.
- Sound waves in the plasma after the bubbles have collided but before expansion has dissipated the kinetic energy in the plasma.
- Magnetohydrodynamic (MHD) turbulence in the plasma forming after the bubbles have collided

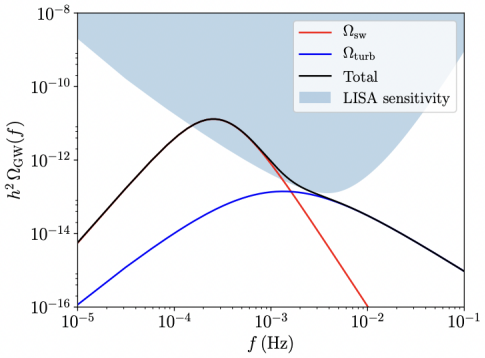


**Figure 10**. Example of a GW power spectrum for a thermal PT with $v_w = 0.44$, $\alpha = 0.084$, $H_*/\beta = 0.1$ and $T_* = 180\,\text{GeV}$. The power spectrum is compared to a sensitivity curv obtained for a LISA-like configuration. Taken from 1705.01783.

The stochastic background is the sum of these processes

$$\Omega_{\rm gw} = \Omega_\phi + \Omega_{\rm sw} + \Omega_{\rm turb} \tag{4.81}$$

The bubble wall contribution is generically subdominant, it may only dominate for supercooled/cold transitions, or for runaway bubble walls with a velocity approaching the speed of light – in both cases the transfer of energy to the plasma is small. The plasma will be accelerated and heated by the expanding bubble; the gravitational wave signal will depend on the kinetic energy of the plasma. Hydrodynamica simulations can give more accurate estimates than above. The input is a set of phenomenological parameters describing the system. These are the temperature $T_* \approx T_n$, the bubble wall velocity $v_w$, and the time-scale of the transition $\beta$. In addition, parameters describing the energy content: the ratio of vacuum energy density released in the transition compared to the total energy density in the plasma, and the fraction of vacuum energy density that gets converted into bulk motion of the fluid and into gradient energy of the Higgs field, important to determine the relevant contributions to the total signal.

$$\alpha = \frac{\rho_{\rm vac}}{\rho_{\rm rad}}, \quad \kappa_v = \frac{\rho_v}{\rho_{\rm vac}}, \quad \kappa_\phi = \frac{\rho_\phi}{\rho_{\rm vac}} \tag{4.82}$$

at the time of emission. Given an actual model, these parameters can then be mapped to the Lagrangian parameters. For $\beta, \alpha$ this is rather straightforward, but it is much harder to dermine the others, as they will depend on the bubble interactions with the plasma.

**EW baryogenesis** Redo Can the GW signal be used to test models of EW baryogenesis? Unfortunately, this seems hard given sensitivity of upcoming experiments. The GW signal is largest for strong transition with large, relativistic bubble wall velocities. This maximises the energy that can be transferred to kinetic energy of the plasma, available for GW production.

Baryogenesis on the other hand is most efficient for smaller bubble wall velocities $v_v \sim 0.1$, the efficiency reduces fast for velocities larger than the sound speed in the plasma $c_s = 1/\sqrt{3}$. The reason is that the asymmetry between left-handed particles and antiparticles is created in the bubble wall region where CP is violated. This assymmetry has to defuse into the symmetric phase, where the sphaleron transition can convert it in a baryon assymetry. If the bubble wall moves faster than the speed of sound, there is no signifanct diffussion in the symmetric phase, as the particles are overtaken by the bubble. Sphalerons have ample time to interact, and the baryon asymmetry will be small. This gives an upper bound on the bubble wall velocity for efficient baryogenesis. For very small velocities the system is at all times close to equilibrium and no large assymetry is produced either.

# A FLWR cosmology

Modern cosmology is grounded on the "cosmological principle": nobody is at the center of the universe, and the cosmos viewed from any point looks the same as from any other point. It is the Copernican principle – we are not the center of the solar system – taken to the extreme. It implies that the universe (on large scales) is isotropic and homogeneous (as seen by a freely falling observer), and is invariant under spatial translations and rotations. The cosmic microwave background (CMB) and large scale structure surveys confirm the homogeneity and isotropy of the universe on *large scales* $> 100$ Mpc (the observable patch of our universe is $\sim 3000$Mpc).

An isotropic and homogenous universe is described by the Friedman-Robertson-Walker (FRW) metric:

$$\mathrm{d}s^2 = -\mathrm{d}t^2 + a(t)^2 \left[ \frac{\mathrm{d}r^2}{(1-kr^2)} + r^2 \left( \mathrm{d}\theta^2 + \sin^2\theta \mathrm{d}\varphi^2 \right) \right] = g_{\mu\nu} \mathrm{d}x^\mu \mathrm{d}x^\nu \tag{A.1}$$

with $a(t)$ the time-dependent cosmic scale factor. $\mathrm{d}s$ measures the proper distance between two points in spacetime separated by $\mathrm{d}x^\mu$. The constant $k = -1$, 0, 1 for an open, flat, or closed universe respectively, corresponding to the 3-dimensional spatial slices being hyperbolic surfaces, flat, or 3-spheres. To write the metric in the above form, the freedom to redefine $r \to \lambda r$ has been used to normalize $|k| = 1$ for curved universes.

$\{r, \theta, \varphi\}$ are called comoving coordinates, a particle initially at rest in these coordinates remains at rest, i.e. $\{r, \theta, \varphi\}$ remains constant. The physical separation between freely moving particles at $(t, 0)$ and $(t, r)$ is

$$d(r,t) = \int \mathrm{d}s = a(t) \int_0^r \frac{\mathrm{d}r}{\sqrt{1-kr^2}} = a(t) \times \begin{cases} \sinh^{-1} r, & k = -1, \\ r, & k = 0, \\ \sin^{-1} r, & k = 1. \end{cases} \tag{A.2}$$

Thus physical distances and wavelengths scale $\lambda \propto a$, and momenta $p \propto a^{-1}$. The distance increases with time in an expanding universe ($\dot{a} > 0$):

$$\dot{d} = \frac{\dot{a}}{a} d \equiv H d, \tag{A.3}$$

with $H(t)$ the Hubble parameter or constant (to indicate it is independent of spacial coordinates). The above is nothing but Hubble's law: galaxies recede from each other with a velocity that is proportional to the distance. Hubble's law is borne out by observations; the present day measured Hubble parameter is $H_0 \sim 70$ km/sec/Mp. A subscript 0 denotes the present day value of the corresponding quantity.

A freely moving particle will eventually come at rest in comoving coordinates as its momentum is red shifted $p \propto a^{-1}$ to zero. The expansion of the universe creates a kind of dynamical friction for everything moving in it. It will be useful to define comoving distance and momenta, with the expansion factored out, via

$$\lambda_{\mathrm{com}} = \lambda_{\mathrm{phys}}/a(t), \qquad k_{\mathrm{com}} = a(t) k_{\mathrm{phys}}. \tag{A.4}$$

Motion w.r.t. comoving coordinates is called peculiar motion, it probes the local mass density.

A photon emitted with wavelength $\lambda_{\mathrm{em}}$ from a distant galaxy is red shifted, and observed at present with a longer wavelength $\lambda_0$, given by

$$(1+z) \equiv \frac{\lambda_{\mathrm{em}}}{\lambda_0} = \frac{a_0(t_0)}{a_{\mathrm{em}}(t_{\mathrm{em}})}, \tag{A.5}$$

that is light with red shift $(1+z)$ was emitted when the universe was a factor $(1+z)^{-1}$ smaller. Another way to look at the effects is that from eq. (A.3) photons are red shifted due to the recession velocity of the source.

### A.1 Friedmann equation

In general relativity the metric is a dynamical object. The time evolution of the scale factor in eq. (A.1) is governed by Einstein's equations

$$R_{\mu\nu} - \frac{1}{2} R g_{\mu\nu} = 8\pi G_N T_{\mu\nu} \tag{A.6}$$

with $R$ and $R_{\mu\nu}$ the scalar curvature and Ricci curvature tensor respectively, which are both complicated functions of the metric with up to two metric derivatives. We will use units in which $M_{\rm P}^2 = (8\pi G_N)^{-1} = 1$. The gravitational field, that is the metric of spacetime, is sourced and curved by matter/energy. The energy-momentum tensor is dictated by isotropy and homogeneity to be of the perfect fluid form $T^\nu_\mu = \mathrm{diag}(-\rho, p, p, p)$. Then Einstein's equations reduce to two independent equations

$$H^2 \equiv \left(\frac{\dot{a}}{a}\right)^2 = \frac{\rho}{3} - \frac{k}{a^2} \qquad \text{(Friedmann eq.)} \tag{A.7}$$

$$\frac{\ddot{a}}{a} = -\frac{1}{6}(\rho + 3p) \qquad \text{(Raychaudhuri eq.)} \tag{A.8}$$

The Raychaudhuri equation can also be traded for the continuity equation

$$\dot{\rho} = 3H(\rho + p) \qquad \text{(continuity eq.)} \tag{A.9}$$

which encodes energy conservation; it can also be derived from $\nabla_\nu T^{\mu\nu} = 0$. Equation (A.9) can be viewed as the 1st law of thermodynamics:

$$\mathrm{d}U = -p\mathrm{d}V \quad \Rightarrow \quad \mathrm{d}(\rho a^3) = -p\mathrm{d}(a^3). \tag{A.10}$$

Introduce the equation of state parameter $p \equiv \omega\rho$. Then the continuity equation can be integrated to give

$$\frac{\mathrm{d}\rho}{\rho} = -3(1+\omega)\frac{\mathrm{d}a}{a} \quad \Rightarrow \quad \rho \propto a^{-3(1+\omega)} \tag{A.11}$$

From eq. (A.7), neglecting the curvature term, it then follows

$$a \propto \begin{cases} t^{2/(3(1+\omega))} & \omega \neq -1 \\ \mathrm{e}^{Ht} & \omega = -1 \end{cases} \tag{A.12}$$

This can be derived substituting $a = t^n$ and eq. (A.11) in eq. (A.7), to give $(n/t)^2 = 1/3t^{-3n(1+\omega)}$. This has the solution $n = 2/(3(1+\omega))$ provided $\omega \neq 1$. For $\omega = -1$ then $\rho =$ const. and eq. (A.7) has an exponential solution.

The matter in the universe consists of several fluids $T^\nu_\mu = \sum_i T^{(i)}{}^\nu_\mu$, with $i = \{\gamma, M, \Lambda\}$ for radiation, non-relativistic matter and vacuum respectively. If the energy exchange between them is negligible, it follows that all fluids separately satisfy the continuity equation. We can define an equation of state parameter for each fluid separately $p_i = \omega_i\rho_i$.

- Radiation includes all relativistic species, at present only photons (generically, species are relativistic when $m \ll T$). For radiation $\omega_{\rm rad} = 1/3$ and thus eq. (A.11) gives $\rho_{\rm rad} \propto a^{-4}$. If the universe is *dominated* by radiation, it follows from eq. (A.12) that the scale factor grows $a \propto t^{1/2}$.

- Matter includes all non-relativistic or cold matter, at present baryons, dark matter and neutrinos. For matter $\omega_{\rm mat} = 0$ and thus $\rho_{\rm M} \propto a^{-3}$. If the universe is *dominated* by matter, the scale factor grows $a \propto t^{2/3}$.

- Vacuum energy (a cosmological constant) $\rho_\Lambda$ with $\omega_\Lambda = -1$ remains constant in time. If it *dominates* the universe $a \propto \mathrm{e}^{Ht}$.

Define $\Omega_i = \rho_i/\rho_c$ with $\rho_c = 3H^2$ the critical density. Then the Friedmann equation eq. (A.7) becomes

$$\Omega = \sum_i \Omega_i = 1 + \frac{k}{(aH)^2} \tag{A.13}$$

Thus $\Omega$ is larger, equal, or smaller than unity for an open, flat or closed universe respectively. From observations (CMB data, supernovae, large scale structure, lensing, big bang nucleosynthesis(BBN)) we find for the present values

$$\Omega - 1 \approxeq 0, \quad \Omega_{\rm B} \approxeq 0.05, \quad \Omega_{\rm DM} \approxeq 0.27, \quad \Omega_\gamma \approxeq 8 \times 10^{-5}, \quad \Omega_\Lambda \approxeq 0.68 \tag{A.14}$$

with $B$ and $DM$ denoting baryons and dark matter. Visible matter only makes up a very small part.

### A.2 Thermal history

A species in thermal equilibrium has a phase space density given by the Bose-Einstein and Fermi-Dirac distributions

$$f(\mathbf{p}) = \frac{1}{\exp\left(\omega - \mu\right)/T \mp 1} \tag{A.15}$$

with $\omega = \sqrt{\mathbf{p}^2 + m^2}$ the energy density, $\mu$ the chemical potential and the $-$ $(+)$ sign is for bosons (fermions). If interactions rates $A + B \leftrightarrow C + D$ is in thermal equilibrium the chemical potentials are related $\mu_A + \mu_B = \mu_C + \mu_D$. The number and energy density are given yb

$$n = g \int \frac{\mathrm{d}^3 p}{(2\pi)^3} f(\mathbf{p}), \quad \rho = g \int \frac{\mathrm{d}^3 p}{(2\pi)^3} E(\mathbf{p}) f(\mathbf{p}) \tag{A.16}$$

with $g$ the internal degrees of freedom.

For relativistic degrees of freedom $T \gg m$ this gives

$$n = \frac{g}{2\pi^2} T^3 \int \frac{y^2}{e^y \mp 1} \mathrm{d}y = \frac{g c_n}{\pi^2} \zeta(3) T^3, \quad \rho = \frac{g}{2\pi^2} T^4 \int \frac{y^3}{e^y \mp 1} \mathrm{d}y = \frac{g \pi^2 c_\rho}{30} T^4 \tag{A.17}$$

with $c_n = \{1, \frac{3}{4}\}$ and $c_\rho = \{1, \frac{7}{8}\}$ for bosons and fermions. In the non-relativistic limit $T \ll m$ and neglecting chemical potentials

$$n \simeq g \frac{g}{2\pi^2} \mathrm{e}^{-m/T} (2mT)^{3/2} \int x^2 \mathrm{e}^{-x} \mathrm{d}x = g \left(\frac{mT}{2\pi}\right)^{3/2} \mathrm{e}^{-m/T} \tag{A.18}$$

the same for bosons and fermions, and $\rho = mn$.

The radiation energy density can then be written as

$$\rho_r = \frac{\pi^2}{30} g_*(T) T^4, \tag{A.19}$$

with $g_*$ the relativistic dof in thermal equilibrium with the photons . During radition domination the Hubble constant scales as $H^2 = \rho_r/3 \propto T^4$. Another useful quantity is the entropy density $s = S/\mathcal{V} = (E + p\mathcal{V})/T = (\rho + p)/T$. For a relativistic species $p = \rho/3$ and $s = \frac{4}{3}(\rho/T)$. The total entropy density is

$$s = \frac{2\pi^2}{45} g_{*S}(T) T^3 \tag{A.20}$$

with $g_{*S}$ the dof contributing to the entropy (for species in thermal equilibrium $g_{*S} = g_*$). Entropy conservation implies that

$$S = a^3 s \propto g_{*S}(T) T^3 a^3 = \text{const.} \quad \Rightarrow a \propto (g_{*S} T)^{-1} \tag{A.21}$$

If no number densities are being created/destroyed the ratio $Y_i = n_i/s$ remains constant, and is therefore often used in Boltzmann equations.

Reaction drop out of equilibrium if the interaction rate becomes slow compared to the Hubble constant $\Gamma \lesssim H$, and interactions can no longer keep up with Hubble expansion and less than one scattering in per Hubble time will occur. The interaction rate for particle $A$ in the reaction $A + A \to X$ can be estimated as $\Gamma \sim n_A \sigma v$ with $\sigma$ the cross section and $v$ the velocity of incoming particles (for relativistic particles $v = 1$).

## References


[1] J.M. Cline, *Baryogenesis*, in *Les Houches Summer School - Session 86: Particle Physics and Cosmology: The Fabric of Spacetime*, 9, 2006 [hep-ph/0609145].

[2] D. Bodeker and W. Buchmuller, *Baryogenesis from the weak scale to the grand unification scale*, *Rev. Mod. Phys.* **93** (2021) 035004 [2009.07294].

[3] A. Riotto, *Theories of baryogenesis*, in *ICTP Summer School in High-Energy Physics and Cosmology*, pp. 326–436, 7, 1998 [hep-ph/9807454].

[4] W. Buchmuller, P. Di Bari and M. Plumacher, *Leptogenesis for pedestrians*, *Annals Phys.* **315** (2005) 305 [hep-ph/0401240].

[5] G.F. Giudice, A. Notari, M. Raidal, A. Riotto and A. Strumia, *Towards a complete theory of thermal leptogenesis in the SM and MSSM*, *Nucl. Phys. B* **685** (2004) 89 [hep-ph/0310123].

[6] M. Drewes, B. Garbrecht, P. Hernandez, M. Kekic, J. Lopez-Pavon, J. Racker et al., *ARS Leptogenesis*, *Int. J. Mod. Phys. A* **33** (2018) 1842002 [1711.02862].

[7] M. Laine and A. Vuorinen, *Basics of Thermal Field Theory*, vol. 925, Springer (2016), 10.1007/978-3-319-31933-9, [1701.01554].

[8] M. Quiros, *Field theory at finite temperature and phase transitions*, *Acta Phys. Polon. B* **38** (2007) 3661.

[9] S. Coleman, *Aspects of Symmetry: Selected Erice Lectures*, Cambridge University Press, Cambridge, U.K. (1985), 10.1017/CBO9780511565045.

[10] D.E. Morrissey and M.J. Ramsey-Musolf, *Electroweak baryogenesis*, *New J. Phys.* **14** (2012) 125003 [1206.2942].

[11] M. Trodden, *Electroweak baryogenesis*, *Rev. Mod. Phys.* **71** (1999) 1463 [hep-ph/9803479].

[12] A. Mazumdar and G. White, *Review of cosmic phase transitions: their significance and experimental signatures*, *Rept. Prog. Phys.* **82** (2019) 076901 [1811.01948].

[13] J.I. Kapusta and C. Gale, *Finite-temperature field theory: Principles and applications*, Cambridge Monographs on Mathematical Physics, Cambridge University Press (2011), 10.1017/CBO9780511535130.

[14] S.R. Coleman, *The Fate of the False Vacuum. 1. Semiclassical Theory*, *Phys. Rev. D* **15** (1977) 2929.

[15] A.D. Linde, *Decay of the False Vacuum at Finite Temperature*, *Nucl. Phys. B* **216** (1983) 421.